Title	Phenotypic and functional heterogeneity of human intermediate monocytes based on HLA-DR expression
Author(s)	Connaughton, Eanna P.; Naicker, Serika; Hanley, Shirley A.; Slevin, Stephanie M.; Eykelenboom, John K.; Lowndes, Noel F.; O'Brien, Timothy; Ceredig, Rhodri; Griffin, Matthew D.; Dennedy, Michael C.
Publication Date	2018-03-05
Publication Information	Connaughton, Eanna P, Naicker, Serika, Hanley, Shirley A, Slevin, Stephanie M, Eykelenboom, John K, Lowndes, Noel F, O'Brien, Timothy, Ceredig, Rhodri, Griffin, Matthew D, Dennedy, Michael C. (2018). Phenotypic and functional heterogeneity of human intermediate monocytes based on HLA-DR expression. Immunology & Cell Biology, 96(7), 742-758. doi:10.1111/imcb.12032
Publisher	Wiley
Link to publisher's version	https://doi.org/10.1111/imcb.12032
Item record	http://hdl.handle.net/10379/15013
DOI	http://dx.doi.org/10.1111/imcb.12032

PHENOTYPIC AND FUNCTIONAL HETEROGENEITY OF HUMAN INTERMEDIATE MONOCYTES BASED ON HLA-DR EXPRESSION

Connaughton EP, Naicker S, Hanley SA, Slevin SM, Eykelenboom JK, Lowndes NF, O'Brien T, Ceredig R, Griffin MD, Dennedy MC

Running title: Human intermediate monocyte heterogeneity

Corresponding author: Michael Conall Dennedy, MD, PhD, FRCPI, Consultant Endocrinologist / Senior Lecturer in Therapeutics,

Address for correspondence: Discipline of Clinical Pharmacology & Therapeutics, 3.13 Lambe Institute for Translational Medicine, National University of Ireland, Galway, Galway, Rep. of Ireland

Tel: +353 91 465371

Email: michael.dennedy@nuigalway.ie

Key terms: Chemokine, Adhesion Molecule, Scavenger Receptor, Migration, Lipoproteins, Obesity, Atherosclerosis

Word count: 5917 (36,548 Characters)

Funding sources: Health Research Board of Ireland, Molecular Medicine Ireland, Science Foundation Ireland, Health Services Executive of Ireland.

AUTHORSHIP

Authors

Eanna P Connaughton PhD[1]	Research Fellow
Serika Naicker MSc[1]	Research Fellow
Shirley A Hanley PhD[1]	Senior Technical Officer
Stephanie M. Slevin PhD[1]	Research Fellow
John K. Eykelenboom, PhD[2]	Research Fellow
Noel F. Lowndes, PhD[2]	Professor
Timothy O'Brien MD, PhD[1]	Consultant / Professor
Rhodri Ceredig MD, PhD[1]	Professor
Matthew D Griffin MB, BCh, DMed[1]	Consultant / Professor
Michael C Dennedy MD, PhD[1,3]	Consultant / Senior Lecturer

Author Affiliations: [1]Regenerative Medicine Institute (REMEDI) at CÚRAM Centre for Research in Medical Devices, School of Medicine, College of Medicine, Nursing and Health Sciences, National

University of Ireland, Galway, Newcastle Road, Galway, Co. Galway, Ireland. [2] Centre for Chromosomal Biology, Department of Biochemistry, School of Natural Sciences, College of Science, National University of Ireland, Galway. [3] Discipline of Pharmacology and Therapeutics, Lambe Institute for Translational Medicine, School of Medicine, National University of Ireland, Galway.

Author Contributions: EPC, SN, SAH, SS, JKE, NFL, TOB, RC, MDG, MCD: Experimental design and execution. EPC, SN, JKE, NFL, TOB, RC, MDG, MCD data analysis and interpretation. EPC, MDG, MCD Manuscript preparation. SN:, data analysis and interpretation, preparation of figures. SS: Experimental execution, data analysis and preparation of figures.

ABSTRACT

Human blood monocytes are sub-classified as classical, intermediate and non-classical. In this study, it was shown that conventionally-defined human intermediate monocytes (IM) can be divided into two distinct subpopulations with mid- and high-level surface expression of HLA-DR (referred to as DR^{mid} and DR^{hi}IM). These IM subpopulations were phenotypically and functionally characterized in healthy adult blood by flow cytometry, migration assays and lipoprotein uptake assays. Their absolute numbers and proportions were then compared in blood samples from obese and non-obese adults. DR^{mid} and DR^{hi}IM differentially expressed several proteins including CD62L, CD11a, CX3CR1 and CCR2. Overall, the DR^{mid}IM surface profile more closely resembled that of classical monocytes while DR^{hi}IM were more similar to non-classical. However, in contrast to classical monocytes, DR^{mid}IM migrated weakly to CCL2, had reduced intracellular calcium flux following CCR2 ligation and favored adherence to TNF-α-activated endothelium over transmigration. In lipid uptake assays, DR^{mid}IM demonstrated greater internalization of oxidized and acetylated low density lipoprotein than DR^{hi}IM. In obese compared to non-obese adults, proportions and absolute numbers of DR^{mid}, but not DR^{hi}IM, were increased in blood. The results are consistent with phenotypic and functional heterogeneity within the IM subset that may be of specific relevance to lipoprotein scavenging and metabolic health.

INTRODUCTION

Monocytes are circulating innate immune cells that migrate to tissues in response to injury and infection where they principally act as effector cells but may also differentiate into macrophages and dendritic cells[1]. The hallmark functional feature of monocytes is their rapid, adaptable response to circulating and micro-environmental cues and their ability to interact with the endothelium to modulate the interface between the circulation and tissues. Consistent with this biological plasticity, monocytes express a broad range of surface receptors involved in diverse functional activities including migration, pattern recognition, scavenging, phagocytosis, antigen presentation and interaction with lymphocytes[2]. Hence, monocytes have been shown to display considerable phenotypic and functional heterogeneity depending on their environment and it is now accepted that they are likely to commit to specific activation phenotypes and differentiation pathways while circulating[3,4].

Based on flow cytometric characteristics exhibited by circulating human monocytes, a consensus on classification of these cells recommends categorization into three subsets based on surface expression of CD14 and CD16: classical ($CD14^+/CD16^-$), intermediate ($CD14^+/CD16^+$) and non-classical ($CD14^-/CD16^{++}$)[5-7]. Studies aimed at identifying the roles for each of these monocyte subsets demonstrate that classical monocytes are pro-inflammatory, readily phagocytose bacteria and are primed to migrate to inflamed/damaged tissues[2,8]. In line with this, they highly express markers of migration, such as CCR2 and CD62L, while demonstrating low expression of CX3CR1[2,8]. Non-classical monocytes are less likely to migrate into tissues but rather crawl along the endothelium to act as “patrollers” of the endothelial surface. Their high expression of CX3CR1, as well as LFA-1, modulates this activity while lower expression of CCR2 may limit trans-endothelial migration[1,2]. Non-classical monocytes may represent the “first responder” innate immune cell, which polices the endothelium and recruits classical monocytes and neutrophils in response to insult[9]. They also have considerable antigen presentation capacity[2,8,10].

Studies of human intermediate monocyte function have provided more variable findings. The intermediate surface phenotype has been characterized as

$CD14^{+}/CD16^{+}/CCR2^{mid}/CX3CR1^{mid}/CD62L^{mid}$ and the functional characteristics are considered to overlap with those of classical and non-classical monocytes[2,10]. A consistent observation across several studies is the high phagocytic activity of intermediate monocytes[2,10,11]. However, data pertaining to other functional roles, such as antigen presentation and T-cell interaction have not been as consistent. While some studies report intermediate monocytes to express a pro-inflammatory phenotype, releasing high quantities of TNFα and IL-1β following toll-like receptor (TLR) stimulation, others have demonstrated the converse[2,8,12]. Hierarchical clustering of intermediate monocyte gene expression profiles has variously indicated that they cluster more closely with classical[2] or with non-classical monocytes[8,10]. The lack of an equivalent intermediate monocyte subset in animal models has added further difficulty to their characterization. It has been suggested that the intermediate monocyte subset represents a transitional state between the more immature classical and more mature non-classical subsets[10]. This proposed translational pathway has recently been substantiated. A study by Patel et al, 2017[13], reported that classical human monocytes that were grafted into a humanized mouse were able to differentiate sequentially into intermediate and non-classical monocytes. This proposed pathway has recently been substantiated by Patel et al, 2017[13] who applied human *in vivo* deuterium labelling and a humanized mouse model to demonstrate sequential maturation of bone marrow-release classical monocytes in the circulation to intermediate and non-classical monocytes.

It is important that the characteristics of intermediate monocytes are better understood, particularly given their likely clinical significance. For example, several reports have documented the expansion of intermediate monocytes in a range of conditions associated with chronic inflammation such as chronic kidney disease[14], inflammatory bowel disease[15,16] and type 2 diabetes mellitus[17]. This altered circulating monocyte repertoire has been postulated to contribute to chronic vascular damage, endothelial dysfunction and atherosclerosis[14,18]. However, the true clinical significance of these findings cannot be fully interpreted in the context of current uncertainty regarding intermediate monocyte origin and function. To better understand intermediate monocyte heterogeneity in healthy humans, we performed a series of studies designed to evaluate their surface phenotype and functional activity in terms of migratory properties and ability to internalize modified and unmodified

lipoproteins. The results indicate that the intermediate monocyte subset, as currently defined, contains sub-populations with phenotypic and functional heterogeneity that are distinguishable based on surface expression of the class II MHC protein, HLA-DR. Furthermore, we find that intermediate monocyte expansion associated with obesity is confined to one of two such subpopulations.

RESULTS

HLA-DR expression levels distinguish two subpopulations of human intermediate monocytes: In order to quantify and functionally characterize human monocytes and their subpopulations in PBMCs isolated from healthy adults, a 4-parameter flow cytometry gating strategy was developed and validated for accuracy against an 8-parameter gating strategy which included staining for additional monocyte inclusion/exclusion markers. As shown in Figure 1A&B, these two gating strategies culminated in CD14/CD16 profiles that were closely consistent with those reported by others and allowed for subdivision of total monocytes into the accepted convention of classical, intermediate and non-classical[2,19-22]. By both gating strategies, monocytes falling within the intermediate monocyte ($CD14^{++}/CD16^{+}$) gate consistently separated into two distinct subpopulations based on mid-and high-level expression of HLA-DR (hereafter referred to as DR^{mid} and DR^{hi} intermediate monocytes) (Figure 1A&B). Importantly, proportions of classical, DR^{mid} intermediate, DR^{hi} intermediate and non-classical monocytes among PBMC samples from 8 healthy adults (5 female and 3 male), did not differ between the 4-parameter and 8-parameter gating strategies (Figure 1C).

Back-gating against the currently recognized CD14 vs. CD16 plots confirmed that both DR^{mid} and DR^{hi} intermediate monocytes fell clearly within the intermediate monocyte gate and were not explained by “spill over” from classical or non-classical subsets. DR^{hi} intermediate monocytes showed a greater range of CD16 expression but there was considerable overlap between both subpopulations when identified within CD14 vs. CD16 plots (Supplementary Figure 1A). Morphological properties of the monocyte subpopulations, compared using scatter characteristics, showed that non-classical monocytes represented the smallest (based on forward scatter) and least granular (based on side scatter) monocyte subpopulation. DR^{mid} intermediate monocytes were the most granular monocyte while DR^{hi} intermediates were the largest (Supplementary Figure 1B).

Expression of chemokine receptors and adhesion molecules differs between the DR^{mid} and DR^{hi} intermediate monocyte subpopulations: Investigation of cell surface markers associated with chemokinesis, endothelial adhesion and migration was carried out across all monocyte

subpopulations using the 4-parameter gating strategy shown in Figure 1A. Significant differences in surface expression of the chemokine receptors CCR2 and CX3CR1, but not CCR5, CCR6, and CXCR4, were demonstrated between DR^{mid} and DR^{hi} intermediate monocytes (Figure 2A-E). Differences in surface expression of specific adhesion molecules between DR^{mid} and DR^{hi} intermediate monocytes were also observed. DR^{hi} intermediate monocytes had higher expression of the integrin chains CD11a, CD11b and CD11c (Figure 2: F-I), while the DR^{mid} intermediate subpopulation had higher expression of CD62L (L-selectin) and P-selectin glycoprotein type-1 (PSGL-1) (Figure 2J&K). The surface phenotypes of classical and DR^{mid} intermediate monocytes for the functional markers analyzed were closely similar with no differences in expression levels of CCR2, CCR5, CCR6, CXCR4, CD11b, CD11c, CD49b, CD62L, PSGL-1 and CD31. Nonetheless, the surface levels of CX3CR1 and CD11a were slightly but significantly higher on DR^{mid} intermediate compared to classical monocytes (Figure 2A&F). The surface phenotypes of DR^{hi} intermediate and non-classical monocytes also had notable similarities, including higher CX3CR1, CD11a and CD11c and lower CCR2 and CD62L than the classical and DR^{mid} intermediate sub-populations. However, of the 12 markers analyzed, 7 had different surface expression levels on DR^{hi} intermediate compared to non-classical monocytes. The relative expression levels of chemokine receptors and adhesion molecules for classical and non-classical monocytes were in line with previously published findings[2,10]. These phenotypic analyses provide evidence for distinct DR^{mid} and DR^{hi} monocyte subpopulations within the human intermediate monocyte population of healthy adults. They also demonstrate that classical and DR^{mid} intermediate monocytes express very similar surface profiles for chemokine receptors and adhesion proteins, albeit with some subtle differences. The surface phenotype DR^{hi} intermediate monocytes more closely resembles that of non-classical monocytes but with differential expression of multiple chemokine receptors and adhesion proteins.

Monocyte subpopulations differ in adhesion and transmigration properties in response to chemokines and across activated endothelium: Migration of isolated monocytes in response to CCL2 (MCP-1), CCL8 (MCP-2) and CCL7 (MCP-3) was investigated using a transwell assay system. Overall, there was a higher migration rate of classical monocytes in response to all three chemokines when compared with the non-chemokine control, with the highest index of migration occurring in

response to CCL7 (9.9 ± 4.5; P < 0.001) (n=8) followed by CCL2 (5.2 ± 1.1; P < 0.01) (n=8) and CCL8 (3.6 ± 1.7; P < 0.05) (n=8) (Figure 3A&B). In contrast, chemokine-driven migration of both intermediate monocyte subpopulations and of non-classical monocytes did not reach statistical significance in comparison with the no-chemokine control. Furthermore, the DR^{mid} and DR^{hi} intermediate sub-populations did not significantly differ in their migration responses to the three MCP family chemokines.

To mimic monocyte migration across an endothelial layer, healthy adult PBMCs were added to transwells coated with human aortic endothelial cells (HAEC), in either a resting or TNFα-activated state (Supplementary Figure 2). Following 1 hour of culture, the floating (non-adherent), adherent and transmigrated fractions of each monocyte subpopulation were quantified (Figure 3C). In these assays, TNFα-induced activation of HAEC was associated with lower proportions of all four monocyte sub-populations within the floating fraction. This was accompanied by a proportionate increase in the adherent fractions for each subpopulation when compared with co-cultures using resting endothelium (Figure 3C). DR^{hi} intermediate and non-classical monocytes demonstrated the greatest proportional decrease in the floating cells accompanied by the highest proportional increase in adherent cells in the presence of TNFα-activated endothelium. Of the four monocyte subpopulations, only classical monocytes had a significant proportional increase in transmigrated cells in the presence of endothelial activation (Figure 3C).

Classical and DR^{mid} intermediate monocytes differ in their intracellular calcium flux following CCL2 ligation and in their RGS protein expression profiles:

Striking among the results described above was the fact that, in comparison to classical monocytes, DR^{mid} Intermediate monocytes had lower migration rate in response to MCP family chemokines as well as lower transmigration through and higher adhesion to activation endothelium despite similar surface expression of CCR2 and various adhesion proteins (as shown in Figure 2). To investigate whether this observation represented a difference in G-protein coupled receptor (GPCR) signaling events following CCR2 ligation by classical and DR^{mid} intermediate monocytes, a flow cytometry-based assay was devised by which intracellular calcium flux (Ca[i])[23] could be simultaneously

quantified in all 4 monocyte subpopulations during a 2-minute time period following exposure to CCL2. This assay was then applied to freshly-isolated PBMC from 4 healthy adults. As shown in Figure 3, only classical and DR^{mid} intermediate monocytes demonstrated a significant peak in Ca[i] in response to CCL2 which then gradually declined to baseline (Figure 4A&B). When the data were expressed as an index, the values for CCL2-induced Ca[i] were significantly higher than vehicle-only control values for classical and DR^{mid} intermediate but not for DR^{hi} intermediate and non-classical monocytes (Figure 4C). Comparing CCL2-induced Ca[i] across the four monocyte sub-populations, classical monocytes displayed the highest value (1.9±0.1), followed by DR^{mid} intermediate (1.6±0.06), DR^{hi} intermediate (1.2±0.07) and non-Classical (1.1±0.03) monocytes (Figure 4D).

These results suggested that the intensity of CCR2-mediated proximal signaling following CCL2 ligation was reduced in DR^{mid} intermediate compared to classical monocytes. We next sought evidence for differential expression among the monocyte sub-populations of members of the regulator of G protein signaling (RGS) family which have been reported to negatively regulate chemokine receptor signaling in human monocytes and other immune cells[24-27]. Classical, DR^{mid} intermediate, DR^{hi} intermediate and non-classical monocytes were sorted by FACS to a high level of purity (Supplementary Figure 3) from freshly isolated PBMC of 7 healthy adults. Individual sorted sub-populations were analyzed by qRT-PCR for relative expression of mRNAs encoding *RGS1*, *2*, *12*, *18* and *FCGR3b* (CD16). For 5/7 sorts, all target mRNAs from all 4 defined monocyte populations were successfully quantified. For the other 2 sorts, all mRNAs were quantified from classical and DR^{mid} intermediate monocytes only. As shown in Figure 5A-E, mRNA levels for *RGS1* and *RGS2* were significantly higher in DR^{mid} intermediate compared with classical monocytes. In the case of RGS1, the expression level was further increased in DR^{hi} intermediate monocytes but reduced again in non-classical monocytes (Figure 5A). In the case of RGS2, there was no further increase in DR^{hi} intermediate and non-classical compared with DR^{mid} intermediate monocytes (Figure 5B). Expression levels of *RGS12* and *18* did not differ between classical and DR^{mid} intermediate monocytes but were, notably, highest in the DR^{hi} intermediate sub-population. The mRNA levels for *FCG3RB* demonstrated, as expected, sequentially higher expression across the four sub-populations. Taken together, the results for CCL2-mediated Ca[i] analysis and RGS1 and RGS2

expression were in keeping with the observed differences between DR^{mid} intermediate and classical monocytes in migratory responses despite their similar surface expression of CCR2.

ApoB lipoprotein uptake differs across human circulating monocyte subpopulations and is highest in the DR^{mid} intermediate subgroup.

In the setting of hypercholesterolemia, unregulated scavenging of modified low-density lipoproteins (LDL) by monocytes adherent to vascular endothelium contributes to chronic vascular damage and atherosclerosis[28-31]. In flow cytometry analyses of healthy adult PBMC, surface expression of the oxLDL scavenger CD36, the acLDL scavenger SCAR-A and the native LDL receptor (LDL-R) (Figure 6A) was found to be highest on classical and DR^{mid} intermediate monocytes. Nonetheless, expression of each receptor was also significantly higher on DR^{hi} intermediate compared with non-classical monocytes.

In lipoprotein uptake assays, all monocyte subpopulations demonstrated similar internalization of non-modified LDL. Consistent with their scavenger receptor expression, however, uptake of the modified lipoproteins oxLDL and acLDL (Figure 6B) was higher in classical and DR^{mid} intermediate monocytes compared with DR^{hi} intermediate and non-classical monocytes. Migration of each monocyte subpopulation in response to oxLDL and LDL across a 3 µM pore-size membrane was quantified. In comparison with control conditions, the migration of DR^{mid} intermediate monocytes was significantly increased in response to oxLDL ($p=0.05$) and LDL ($p=0.01$). This was in contrast to all other monocyte subpopulations, none of which significantly increased their migration rate in response to lipoprotein (Figure 6C). Incubation with LDL, oxLDL and acLDL did not result in altered monocyte expression of CD16 (data not shown).

Circulating numbers of DR^{mid} intermediate monocytes are increased in obesity

Increased numbers and/or proportions of CD16^{+} monocytes have been reported in blood samples from adults with obesity in comparison to those with normal adiposity[32-34]. To investigate the clinical relevance of our HLA-DR-based sub-categorization of intermediate monocytes, the monocyte repertoires of adults with obesity (BMI > 30 kg/m^2) were compared with those of healthy, non-obese

adults. Relevant characteristics of the two groups are summarized in Table 1. Although there were expected differences in relation to fasting lipid parameters and glycosylated hemoglobin (HbA1c), the obese subjects were all non-diabetic and normotensive and did not meet criteria for metabolic syndrome. The obese group had a higher proportion of females (57% vs. 45%) and older median age (39.5 vs. 31 years) than the non-obese group but these differences were not statistically significant (Table 1).

Total circulating monocyte numbers did not differ between non-obese and obese subjects (Figure 7A). However, proportions and absolute numbers of intermediate monocytes were significantly higher in obese subjects with an accompanying proportionate reduction in classical monocytes (Figure 7B). Strikingly, as shown in Figure 7C, the intermediate monocytosis of obese subjects was entirely explained by increased numbers and proportions of the DR^{mid} intermediate subpopulation. Despite their altered monocyte repertoire, the individual monocyte sub-populations of obese subjects did not differ from those of non-obese subjects in regard to surface expression levels of CCR2, CD36, CD91 (LRP-1), CD162 (PSGL-1), CD163 and TLR4 (Supplementary Figure 4).

DISCUSSION

In this detailed analysis of human monocytes, we describe two subpopulations of intermediate monocytes with differential expression of HLA-DR, which had a number of distinct phenotypic and functional characteristics. Furthermore, only one of the two subpopulations was numerically increased in blood samples from obese adults with “intermediate monoctytosis”. These intermediate subpopulations, referred to as DR^{mid} and DR^{hi} intermediate monocytes, demonstrated differential patterns of chemokine receptor, adhesion molecule and lipoprotein/scavenger receptor expression. DR^{hi} intermediate monocytes had higher surface expression of adhesion molecules such as CD11a (LFA-1) and the chemokine receptor CX3CR1, associated with endothelial adhesion and patrolling. DR^{mid} intermediate monocytes, on the other hand, highly expressed CCR2 and CD62L but not CX3CR1. Also characteristic of DR^{mid} compared with DR^{hi} intermediate monocytes was higher expression of lipoprotein and lipoprotein scavenging receptors. While DR^{mid} and DR^{hi} intermediate monocytes exhibited phenotypic characteristics closer to classical and non-classical monocyte subpopulations respectively, their phenotypic profiles also included distinct differences from both classical and non-classical monocytes, suggesting the possibility of specific biological and pathological roles.

The results of migration and endothelial interaction assays were more closely aligned with the surface phenotype for DR^{hi} than for DR^{mid} intermediate monocytes. In keeping with their low expression of CCR2 and high expression of CX3CR1 and specific integrin chains, DR^{hi} intermediate monocytes demonstrated the highest level of adherence to a TNFα-activated arterial endothelial monolayer but did not significantly migrate toward monocyte chemoattractant protein (MCP) family chemokines or through activated endothelium. Their internalization of modified LDL was also lower than that of classical and DR^{mid} intermediate monocytes. Thus, their functional characteristics were quite similar to those of non-classical monocytes within the same PBMC samples. In contrast, DR^{mid} intermediate monocytes were observed to have lower migratory response to MCP family chemokines as well as greater adhesion to and lower transmigration through activated endothelium compared with classical monocytes, despite similar surface expression of CCR2 and adhesion proteins. This

latter finding may indicate that DR^{mid} intermediate monocytes, while closely resembling classical monocytes on the basis of surface phenotype, have reduced transmigratory responsiveness to CCR2 ligation and, therefore, more lasting attachment to the endothelium under inflammatory conditions. We garnered further evidence for this biologically significant functional difference in assays of CCL2-induced Ca[i] and mRNA quantitation of RGS-family proteins. When a chemokine binds to its cognate GPCR, it triggers a rapid series of intracellular molecular events including calcium release from the endoplasmic reticulum and activation of signaling mediators like phospholipase C, diacylglycerol, calmodulin and protein kinase C. These, in turn, induce phosphorylation of target proteins culminating in cytoskeletal re-arrangement and transmigration[23,35]. Thus, the observation of lower CCL2-induced Ca[i] in DR^{mid} intermediate monocytes compared to classical monocytes within the same PBMC preparations, is consistent with reduced intensity of receptor-proximal signaling events and may explain, at least in part, the limited transmigration responses of DR^{mid} intermediate monocytes to chemokine and activated endothelium-derived stimuli. Although further experiments will be required to fully dissect the changes that occur in chemokine-associated signaling and migration as classical monocytes transition to intermediate monocytes (and as intermediate transition to non-classical), our finding of differential expression of mRNAs encoding multiple RGS proteins, which function as negative regulators of proximal GPCR signaling, may provide insight into one important mechanism. These results are in keeping with the previously described expression of RGS1, 2, 12, and 18 by monocyte/macrophagesand, in particular, with reports that RGS1, 2 and 18 may affect CCR2 signaling[24-27,36,37].

In contrast to their reduced migratory responses to MCP family chemokines, DR^{mid} intermediate monocytes were observed to have the highest uptake of modified lipoproteins and were the only monocyte subpopulation to display increased migration toward lipoproteins. Thus, these results suggest that the DR^{mid} intermediate subpopulation is functionally distinct from classical monocytes in having increased responsiveness to lipoproteins and endothelial adhesion along with blunted migratory response to CCR2 ligands. We hypothesize that this subpopulation represents a transitional state of classical monocytes that is characterized by enhanced intravascular scavenging and adhesion. In a broader sense, the findings correlate with the variable phenotypic and functional

profiles that have been described to date for human intermediate monocytes. They may also be consistent with the recent human *in vivo* results of Patel et al., in which expression of a range of surface markers (including HLA-DR, CCR2, CD62L, CX3CR1 and CD36) as well as monocyte subtype identity were shown to flow sequentially from classical to intermediate to non-classical blood monocytes.[13] Studies which have investigated intermediate monocytes defined on the basis of CD14 and CD16 expression have variably shown them to be closer in phenotype or function to either classical [2] or non-classical monocytes[8,10]. Our results indicate that such discordant conclusions may be explained by differences in the relative frequencies of classical-like and non-classical-like subpopulations within the intermediate monocytes studied. Future genome-wide profiling studies of purified intermediate monocyte subpopulations identified by HLA-DR-based or other subdivisions may allow for further clarity in regard to the extent of phenotypic heterogeneity within the currently recognized intermediate subset.

Several studies have shown that human blood monocytes, particularly the intermediate subset, are expanded in various inflammatory disease states[14,15-18]. In particular, the expansion of $CD16^+$ monocyte subpopulations in obesity has been previously documented[32-34,38]. We thus conducted monocyte phenotyping in metabolically healthy obese individuals to determine the contribution of DR^{mid} and DR^{hi} intermediate monocytes to any observed expansion of the intermediate monocyte population. Increased absolute numbers and/or proportions of $CD16^+$ monocytes in blood of obese adults was first reported by Cottam et al. in 2002[32]. This was subsequently confirmed by Rogacev et al. and Poitou et al. who provided additional evidence that circulating $CD16^+$ monocyte numbers correlate with indices of adiposity, systemic inflammation, metabolic health and vascular intimal thickening[33,34]. Consistent with results we present here, these investigators observed that total circulating monocyte numbers were not increased in obesity, likely reflecting a concomitant reduction in classical monocytes[33,34]. However, other details regarding obesity-associated expansion of $CD16^+$ monocytes in these and other studies are less consistent. Some have reported isolated non-classical expansion[33,34] while others have observed expansion of both intermediate and non-classical subsets[38,39] or have not distinguished between the two[32].

Our data, in a cohort of non-diabetic obese adults without severe comorbidity, demonstrate a numerical and proportionate increase of intermediate monocytes without an increase in non-classical monocytes based on a conventional CD14/CD16 gating scheme. We also show, however, that this expansion of intermediate monocytes involves only the DR^{mid} intermediate subpopulation with numbers and proportions of the DR^{hi} subpopulation being no different between the two groups. Given our *in vitro* findings that DR^{mid} intermediate monocytes combine high adhesion to activated endothelium with high avidity for modified lipoproteins, we believe that this novel intermediate subpopulation deserves further consideration as a potential circulating source of atherogenic foam cell precursors. Our additional finding that classical monocytes are proportionately decreased in obese adults raises interesting questions in regard to the relationship between classical and DR^{mid} intermediate monocytes in obesity. It may also indicate that separate triggers and regulatory mechanisms that are not increased in the setting of obesity, determine the rate of further transition of intermediate monocytes toward a non-classical-like state. Thus, the DR^{mid} intermediate subpopulation may represent an immediate transitional state of classical monocytes that is accelerated in response to increased metabolic or inflammatory stress. In keeping with this model of accelerated monocyte transition in the setting of obesity, the increased absolute numbers of circulating DR^{mid} intermediate monocytes that we observed in obese compared to non-obese adults was not accompanied by differences in surface expression levels of receptors involved in lipid uptake/scavenging, inflammatory response and adhesion. However, relative depletion of classical monocytes from the circulation in the setting of obesity could also reflect increased transmigration of this subset into adipose and other tissues.[32].

Our data have been gathered from monocytes collected from healthy individuals and exposed to various stimuli in order to provoke a response. The results reveal novel details in regard to the response of primary human monocyte subsets to chemokine and lipoprotein stimuli and to endothelial activation and also reveal that a specific subpopulation of intermediate monocytes is selectively expanded in adults with obesity. In common with other studies of human monocyte subset phenotype and function, our findings cannot determine the dynamic relationships among the subpopulations nor can they elucidate their individual rates of exchange across different anatomical

compartments but they are compatible with a model of sequential monocyte maturation within the blood stream[13]. *In vivo* studies in mouse suggest that a significant degree of monocyte differentiation occurs within the bone marrow[40] and further differentiation and activation events occurring during the course of endothelial interactions and migration to the tissues[41]. Re-entry of transmigrated monocytes into the circulation has also been documented in rodent models and adds further complexity to the monocyte repertoire as it presents itself in peripheral blood[41,42]. Further studies of human monocyte fate and differentiation using advanced imaging and cell labelling strategies will be required to fully understand the alterations in circulating monocyte repertoire that have been described for obesity and many clinical conditions. Nonetheless, our data contribute to a growing understanding of human monocyte heterogeneity, particularly the intermediate subset, and provide an additional approach to analyzing and interpreting the circulating monocyte repertoire in specific states of health.

METHODS

Study enrolment, data and sample collection

Blood samples from healthy, non-obese and obese adult volunteers were collected at Galway University Hospital and the National University of Ireland, Galway, between March 2010 and June 2015. Healthy, non-obese volunteers were defined as: age > 18 years, BMI < 25 kg/m2, no known chronic illness and not taking any medications or supplements at the time of sampling. Individuals with uncomplicated obesity (OB) were enrolled from a weight management clinic and were defined as: age > 18 years, BMI ≥ 30 kg/m2 without a diagnosis of type 2 diabetes and not taking any regular prescribed medications. Exclusion criteria were: current smoker; inflammatory, hematologic, oncologic, infectious or chronic kidney disease; lower limb ulceration; treatment with systemic glucocorticoids, anti-inflammatory or chemotherapeutic agents. Each participant was recruited into the study under informed, written consent. Subjects meeting enrolment criteria were provided with a participant information leaflet followed by an interview in which concerns were addressed and, finally, signature of the study consent form. Blood was drawn from an arm vein into EDTA-containing 6 mL Vacutainer® tubes (Becton Dickinson) by standard venipuncture technique. Ethical approval was granted following institutional review by the Galway University Hospitals, Human Research Ethics Committee.

Isolation and flow cytometric analysis of peripheral blood mononuclear cells

Peripheral blood mononuclear cells (PBMC) were isolated by gradient centrifugation using endotoxin-free Ficoll Paque® (GE Healthcare, Bucks, UK) [18]. PBMCs were reconstituted in staining buffer (PBS, 2% FBS and 0.05% NaN3) prior to incubation with optimized dilutions of fluorochrome-coupled monoclonal antibodies (mAb). Single staining for compensation of spectral overlap was performed using compensation beads (Thermofisher Scientific, Dublin, IRL) and human cells. All samples were stained with antibodies against CD45, HLA-DR, CD14 and CD16 to identify human monocyte subpopulations according to a validated gating strategy using “fluorescence minus one” controls (Figure 1) [6, 43, 44]. In some experiments, an 8-parameter analysis of monocytes was

performed by the additional staining of PBMC for CX3CR1, CD33 and CD56 (Supplementary Figure 2). To each fully-stained sample, phenotyping mAbs against each surface marker of interest were added at optimized concentrations. Data acquisition was performed on a calibrated FACSCantoII® with FACS DiVa 6.0® acquisition software (BD Biosciences, Oxford, U.K.). Monocyte counts were analyzed using an Accuri® C6 flow cytometer (BD Biosciences), and Countbright Absolute Counting Beads® (Thermofisher Scientific, Dublin, Ireland). FlowJo® V10 analysis software (Tree Star Inc., Ashland, OR) was used for all flow cytometry data analysis.

Migration assays

Transwell inserts with 3.0 μM pore size (Corning, New York, USA) were used in 24-well tissue culture plate format for individual experiments. Migration medium (RPMI [Life Technologies, Carlsbad, CA, USA] supplemented with 0.5% FCS [Lonza, Blackley. U.K.], L-glutamine [Life Technologies] and penicillin/streptomycin [Invitrogen]) was first added to the apical (100 μL) and basal chambers (600 μL) and equilibrated. Freshly isolated PBMCs were re-suspended in 1 mL of migration medium and were kept at 4°C for 40-60 minutes prior to initiating the transmigration assays. Aliquots of 0.5 x 106 serum-starved cells were added to the apical chamber and migration medium containing vehicle control, CCL2, CCL8 or CCL7 (50ng/mL each) (Immunotools, Friesoythe, Germany), low density lipoprotein (LDL) or oxidized LDL (oxLDL) (25 μg/mL each) were added to the basal chamber and incubated at 37°C, 20% O2, 5% CO2 for 60 minutes. Cells from the basal well were retrieved, stained with mAb for identification of monocyte subpopulations, analyzed by flow cytometry and quantified using 20μL of FACs-compatible counting beads (Countbright®; Thermofisher Scientific). Transmigration was represented as an 'index of migration', calculated for each monocyte subpopulation by dividing the number of transmigrated cells in experimental wells (chemokine-containing) by the number of transmigrated cells in the no-chemokine control well.

Human aortic endothelial cells (HAEC) (Promocell, Heidelberg, Germany) were seeded onto fibronectin-coated 3 μM pore size transwell membranes (Corning) in a 12-well tissue culture plate format. Transwell membranes were pre-coated with bovine fibronectin (2 μg/cm2) (Sigma Aldrich, Dublin, Ireland) as previously described. Confluence of HAEC monolayers was confirmed by crystal

violet staining of selected transwell insert membranes (Supplementary Figure 3A). Confluent layers of HAEC from individual transwells were either left unstimulated or were stimulated by addition of human TNF-α (Immunotools) at a final concentration of 2.5 ng/mL for 6 hours at 37°C. Aliquots of stimulated and unstimulated HAEC were lifted by trypsinization, surface stained with mAbs against ICAM-1 and VCAM-1 and analyzed by flow cytometry (Supplementary Figure 3B&C). Isolated monocytes were incubated for 1 hour in a tissue culture incubator at 37°C, 20%, O2, 5% CO2. After incubation, cells from the floating and transmigrated fraction were separately collected. Adherent cells were removed from the inner surface of the transmembrane by brief incubation with trypsin solution (Life Technologies). Proportions of each monocyte subpopulation in the floating, adherent and transmigrated fractions were analyzed using flow cytometry. HAECs were distinguished from monocytes by flow cytometry based on absence of CD45 expression.

Monocyte intracellular calcium flux assay

Freshly-isolated PBMC were in aliquots of 1 x 10^6 cells transferred to FACs tubes and re-suspended to a final volume of 1 mL with Ca^{2+}-free Dulbecco's PBS (D-PBS, Life Technologies California, USA) following which 1.5 μl of 0.2 mM Fluo-4 was added to each tube and mixed. The FACs tubes were sealed with paraffin film, incubated at 37°C, 5% CO_2 for 30 minutes and then centrifuged at 400 RCF for 5 minutes at 20°C. The supernatants were discarded and 100 μL of Ca^{2+}-free D-PBS were added to each tube. The cells were then stained with anti-human CD16-BV450 (eBioscience, UK), anti-human CD14-PerCP, anti-human CD45-APC and anti-human HLA-DR-APC.H7 for 20 minutes at room temperature protected from light. After staining, 1 mL of Ca^{2+}-free D-PBS was added to each tube followed by centrifugation at 400 RCF for 5 minutes at 20°C. The supernatants were removed completely and the cells were re-suspended in 150 μL of Ca^{2+}-free D-PBS then immediately analyzed on a BD FACSCanto II at medium acquisition speed. Events were acquired for 30 seconds in each tube before addition of either 50 ng/mL human CCL2 in 0.1% bovine serum albumin (BSA) (Sigma-Aldrich) in Ca^{2+}-free D-PBS, 10 ng/mL Ionomycin (Life Technologies) (positive control), or 0.1%BSA in Ca^{2+}-free D-PBS alone (negative control). The stimulus solutions were injected into the FACs tube using a modified 500 μl syringe (BD Biosciences). Changes in intracellular calcium over

time were measured by plotting mean fluorescence in the FITC channel against time of acquisition. The data were transformed to kinetic data using the kinetics platform in FlowJo v.7 (Tree Star Inc, Oregon, USA). Calcium flux within individual monocyte subsets was analyzed by gating on each subset based on surface staining for CD45, CD14, CD16 and HLA DR. The results were displayed as an index of Ca^{2+} flux, which was calculated for each sample by dividing the peak fluorescence reached by the average baseline fluorescence during the 30 seconds prior to injection of stimulus.

Monocyte sub-population purification and quantitative RT-PCR

For purification of monocyte sub-populations by fluorescence-activated cell sorting (FACS) from freshly-isolated PBMC, a pre-enrichment step by counter-current centrifugal elutriation was performed. Eight 6 mL EDTA Vacutainer® tubes of blood were drawn from each of 7 healthy volunteers and PBMC were prepared by Ficoll gradient centrifugation as previously described. Buffy coats were transferred to multiple sterile 15 mL Falcon® tubes, the volumes were made up to 10 mL with 2% FCS in PBS and the cells were pelleted by centrifugation at 400 RCF for 5 minutes at 4°C. The supernatants were discarded, the pellets were washed and re-suspended in 5mL each of 2% FCS in PBS then filtered through 30 μm nylon mesh into two 50 mL tubes which were then filled with 2% FCS in PBS. The elutriator (Avanti JE, Beckman Coulter, Pasadena, CA, USA) was accelerated to 2600 rpm with the flow rate set at 25 mL/min using 2% FCS in PBS. When all cells were loaded, 2 x 50 mL fractions were collected in 50 mL tubes. The elutriator was then stopped and 2 further 50 mL 'stop' fractions were collected which contained elutriation-enriched monocytes. The stop fractions were then centrifuged at 400 RCF for 7 minutes, the supernatants were discarded and the cells from each tube were re-suspended in 500 μL of 2% FCS in PBS then pooled together and counted to determine the final cell numbers. Between 3 and 10 x 10^6 elutriation-enriched monocytes were stained in 2% FCS in PBS with anti-human CD16-BV450 (1 μl/10^6 cells) and anti-human HLA-DR-PE (BD Biosciences, UK) (2.5 μL/10^6 cells) with Flow Minus One (FMO) controls prepared at the same time. Antibody incubations were carried out for 20 minutes at 4°C. Sorting was performed on a FACSAria II flow cytometer (BD Biosciences) with dead cells exclusion using Sytox Red® viability dye (Invitrogen, California, USA). Immediately after sorting, the collected cells were pelleted by

centrifugation at 400 RCF for 5 minutes. The supernatants were removed, D-PBS was added and the cells were re-pelleted and re-suspended in cell lysis buffer (Qiagen, Venlo, Netherlands). Total RNA was isolated from the sorted monocyte subsets using an RNeasy Micro Kit (Qiagen) by the manufacturer's suggested protocol for isolation of RNA from PBMC. RNA was quantified using a NanoDrop® 2000 spectrophotometer. All samples used had an A260/A280 ratio of >1.6. First strand cDNA synthesis was carried out using a RevertAid H Minus First Strand cDNA Synthesis Kit (Thermo Fisher Scientific) with an oligo (dT)18 primer mix according to manufacturer's instructions. Before use, cDNA samples were diluted to a concentration of 1 ng/µl, with 2 µl used per well. Quantitative PCR reactions were carried out on a Step One Plus® Real-Time PCR system (Thermo Fisher Scientific) using a SensiFAST SYBR Hi-ROX kit (Bioline, London, UK) and a two-step cycle and data were collected using StepOne software v2.3. SYBR Green I RT-qPCR primers for GAPDH, RGS1, RGS2, RGS12, RGS18, FCG3RB were purchased as pre-designed and validated KiCqStart® primers from Sigma Aldrich. Analysis of relative mRNA expression levels was performed using the relative 2^ΔCT method. GAPDH was used as housekeeping gene for normalisation and classical monocytes were set as the reference sample for each individual subset analysis.

Lipoprotein uptake

Bodipy®-conjugated LDL, oxLDL and acetylated (acLDL) (Thermofisher) preparations were used to measure lipoprotein uptake [45]. PBMCs were incubated in staining buffer with Bodipy®-conjugated lipoproteins, at concentrations of 10 µg/mL [46] for 1 hour at 37°C in a shaking incubator at 50 rpm. Following this, the cell suspensions were immediately cooled to 4°C, stained with phenotyping mAbs as previously described and analyzed by flow cytometry.

Biochemistry Assays

HbA_{1c} was assayed using the Menarini® HA 8160 automated haemoglobin analyser, calibrated to IFCC standardisation, on the principle of reverse phase cation exchange chromatography. The (CV_A%) at a mean HbA_{1c} of 41.6 mmol/mol (Derived DCCT 6%) and 100.5 mmol/mol (Derived DCCT 11.4%) was 2.0 and 1.3% respectively. Total Cholesterol, LDL-C, HDL and triglycerides were

assayed using a Roche analyzer and demonstrated the following %CV: Total Cholesterol 1.6 @ mean value of 3.72mmol/L; LDL-C 1.11 @ mean value of 2.0mmol/L; HDL-C 1.1 @ mean value of 1.0mmol/L; Triglyceride 2 @ mean value of 1.85mmol/L. All assays were performed within a medical testing laboratory accredited to ISO15189:2012 standards.

Data analysis & statistics

Multiple-group comparisons were made using single factor or multivariate analysis of variance (ANOVA/MANOVA). Matched sample and repeated measures comparisons were made using repeated measures ANOVA. All analyses were two tailed and $P < 0.05$ was accepted as statistically significant. Data were tested for assumptions of the statistical tests and transformed for normality using Log10(y) transformation where appropriate. Statistical analyses were performed using Statistics Package for the Social Sciences (SPSS)® V 20 (IBM, Armonk, NY) and GraphPad® Prism V 7.0 (GraphPad Software, San Diego, CA, USA).

ACKNOWLEDGMENTS

The authors acknowledge the kind contribution of time and samples by study participants, as well as the assistance of the nursing and medical staff at the Centre for Diabetes, Endocrinology and Metabolism (CDEM) at Galway University Hospital. We also acknowledge assistance provided by Dr. Paula O'Shea, Consultant Biochemist and staff at the Department of Biochemistry, Galway University Hospital.

EPC, SN and SMS were supported by the Molecular Medicine Ireland Clinical and Translational Research Scholars Programme which was funded by the Irish Government's Programme for Research in Third Level Institutions, Cycle 5 and by NUI Galway. MCD was supported by the Health Services Executive (HSE) of Ireland, Medical Education, Training & Research (METR) Section and the Health Research Board (HRB) of Ireland under the National Specialist Registrar/Senior Registrar Academic Fellowship Program (NSAFP). JKE was partly-funded by grants from the Irish Research Council for Science, Engineering and Technology (IRCSET EMPOWER fellowship) and the Health Research Board (grant number RP2006182N). Funding support was also received from Science Foundation Ireland [Regenerative Medicine Institute Strategic Research Cluster, grant number 09/SRC-B1794; CÚRAM Research Centre, grant number 13/RC/2073 (MDG, TO'B, RC) and Principal Investigators grant numbers 07/IN1/B958 and 13/IA/1954 (NFL)], from the European Commission [Horizon 2020 Collaborative Health Project NEPHSTROM (Novel Stromal Cell Therapy for Diabetic Kidney Disease; grant 634086 (MDG, TO'B)] and from the European Regional Development Fund (all authors).

All flow cytometry and cell sorting experiments were performed in the NUI Galway Flow Cytometry Core Facility which is supported by funds from NUI Galway, Science Foundation Ireland, the Irish Government's Programme for Research in Third Level Institutions, Cycle 5 and the European Regional Development Fund.

CONFLICT OF INTEREST

The authors declare no conflict of interest.

References

1. Auffray C, Sieweke MH, Geissmann F. Blood Monocytes: Development, Heterogeneity, and Relationship with Dendritic Cells. *Annual Review of Immunology* 2009; **27**(1)**:** 669-692.

2. Cros J, Cagnard N, Woollard K *et al.* Human CD14dim Monocytes Patrol and Sense Nucleic Acids and Viruses via TLR7 and TLR8 Receptors. *Immunity* 2010; **33**(3)**:** 375-386.

3. Geissmann F, Manz MG, Jung S *et al*. Development of Monocytes, Macrophages, and Dendritic Cells. *Science* 2010; **327**(5966)**:** 656-661.

4. Soderquest K, Powell N, Luci C *et al.* Monocytes control natural killer cell differentiation to effector phenotypes. *Blood* 2011; **117**(17)**:** 4511-4518.

5. Ziegler-Heitbrock L. The CD14+ CD16+ blood monocytes: their role in infection and inflammation. *Journal of Leukocyte Biology* 2006; **81**(3)**:** 584-592.

6. Ziegler-Heitbrock L, Ancuta P, Crowe S *et al.* Nomenclature of monocytes and dendritic cells in blood. *Blood* 2010; **116**(16)**:** e74-e80.

7. Wong KL, Yeap WH, Tai JJY *et al*. The three human monocyte subsets: implications for health and disease. *Immunologic Research* 2012; 53(1-3):41-57.

8. Zawada AM, Rogacev KS, Rotter B *et al.* SuperSAGE evidence for CD14++CD16+ monocytes as a third monocyte subset. *Blood* 2011; **118**(12)**:** e50-e61.

9. Carlin LM, Stamatiades EG, Auffray C *et al.* Nr4a1-dependent Ly6C low monocytes monitor endothelial cells and orchestrate their disposal. *Cell* 2013; **153**(2)**:** 362-375.

10. Wong KL, Tai JJY, Wong WC *et al.* Gene expression profiling reveals the defining features of the classical, intermediate and nonclassical human monocyte subsets. *Blood* 2011; 118(5):e16-31.

11. Zhou J, Feng G, Beeson J *et al.* CD14(hi)CD16+ monocytes phagocytose antibody-opsonised Plasmodium falciparum infected erythrocytes more efficiently than other monocyte subsets, and require CD16 and complement to do so. *BMC Med* 2015; **13:** 154.

12. Zawada AM, Rogacev KS, Schirmer SH *et al.* Monocyte heterogeneity in human cardiovascular disease. *Immunobiology* 2012**:** 1-12.

13. Patel AA, Zhang Y, Fullerton JN *et al.* The fate and lifespan of human monocyte subsets in steady state and systemic inflammation. *Journal of Experimental Medicine* 2017**;** 214(7): 1913–1923.

14. Rogacev KS, Seiler S, Zawada AM *et al.* CD14++CD16+ monocytes and cardiovascular outcome in patients with chronic kidney disease. *European Heart Journal* 2011; **32**(1)**:** 84-92.

15. Grip O, Bredberg A, Lindgren S *et al*. Increased subpopulations of CD16(+) and CD56(+) blood monocytes in patients with active Crohn's disease. *Inflammatory Bowel Disease* 2007; **13**(5)**:** 566-72.

16. Slevin SM, Dennedy MC, Connaughton EP *et al.* Infliximab Selectively Modulates the Circulating Blood Monocyte Repertoire in Crohn's Disease. *Inflammatory Bowel Disease* 2016; **22**(12)**:** 2863-2878.

17. Yang M, Gan H, Shen Q *et al*. Proinflammatory CD14+ CD16+ monocytes are associated with microinflammation in patients with type 2 diabetes mellitus and diabetic nephropathy uremia. *Inflammation* 2012; **35**(1)**:** 388-396.

18. Rogacev KS, Zawada AM, Emrich I *et al.* Lower Apo A-I and lower HDL-C levels are associated with higher intermediate CD14++CD16+ monocyte counts that predict cardiovascular events in chronic kidney disease. *Arteriosclerosis Thrombosis and Vascular Biology* 2014; **34**(9)**:** 2120-7.

19. Ziegler-Heitbrock L, Ancuta P, Crowe S *et al.* Nomenclature of monocytes and dendritic cells in blood. *Blood* 2010; **116**(16)**:** e74-80.

20. Heimbeck I, Hofer TP, Eder C *et al.* Standardized single-platform assay for human monocyte subpopulations: Lower CD14+CD16++ monocytes in females. *Cytometry. Part A : the Journal of the International Society for Analytical Cytology* 2010; **77**(9)**:** 823-30.

21. Abeles RD, McPhail MJ, Sowter D *et al.* CD14, CD16 and HLA-DR reliably identifies human monocytes and their subsets in the context of pathologically reduced HLA-DR expression by CD14(hi) /CD16(neg) monocytes: Expansion of CD14(hi) /CD16(pos) and contraction of CD14(lo) /CD16(pos) monocytes in acute liver failure. *Cytometry. Part A : the Journal of the International Society for Analytical Cytology* 2012; **81**(10)**:** 823-34.

22. Wong KL, Tai JJ, Wong WC *et al.* Gene expression profiling reveals the defining features of the classical, intermediate, and nonclassical human monocyte subsets. *Blood* 2011; **118**(5)**:** e16-31.

23. Kiselyov K, Shin DM, Muallem S. Signalling specificity in GPCR-dependent Ca2+ signalling. *Cell Signal* 2003; **15**(3)**:** 243-53.

24. Patel J, McNeill E, Douglas G *et al.* RGS1 regulates myeloid cell accumulation in atherosclerosis and aortic aneurysm rupture through altered chemokine signalling. *Nature Communications* 2015; **6:** 6614.

25. Boelte KC, Gordy LE, Joyce S *et al*. Rgs2 mediates pro-angiogenic function of myeloid derived suppressor cells in the tumor microenvironment via upregulation of MCP-1. *PloS one* 2011; **6**(4)**:** e18534.

26. Yuan X, Cao J, Liu T *et al.* Regulators of G protein signaling 12 promotes osteoclastogenesis in bone remodeling and pathological bone loss. *Cell Death and Differentiation* 2015; **22**(12)**:** 2046-57.

27. Shi GX, Harrison K, Han SB *et al*. Toll-like receptor signaling alters the expression of regulator of G protein signaling proteins in dendritic cells: implications for G protein-coupled receptor signaling. *Journal of Immunology* 2004; **172**(9)**:** 5175-84.

28. Febbraio M, Hajjar DP, Silverstein RL. CD36: a class B scavenger receptor involved in angiogenesis, atherosclerosis, inflammation, and lipid metabolism. *The Journal of Clinical Investigation* 2001; **108**(6)**:** 785-791.

29. Charo IF. Macrophage polarization and insulin resistance: PPARgamma in control. *Cell Metabolism* 2007; **6**(2)**:** 96-98.

30. Gerszten RE, Tager AM. The Monocyte in Atherosclerosis — Should I Stay or Should I Go Now? *The New England Journal of Medicine* 2012; **366**(18)**:** 1734-1736.

31. Shapiro H, Pecht T, Shaco-Levy R *et al.* Adipose Tissue Foam Cells Are Present in Human Obesity. *Journal of Clinical Endocrinology & Metabolism* 2013.

32. Cottam DR, Schaefer PA, Fahmy D *et al*. The effect of obesity on neutrophil Fc receptors and adhesion molecules (CD16, CD11b, CD62L). *Obesity Surgery* 2002; **12**(2)**:** 230-5.

33. Rogacev KS, Ulrich C, Blomer L *et al.* Monocyte heterogeneity in obesity and subclinical atherosclerosis. *European Heart Journal* 2010; **31**(3)**:** 369-76.

34. Poitou C, Dalmas E, Renovato M *et al.* CD14dimCD16+ and CD14+CD16+ Monocytes in Obesity and During Weight Loss: Relationships With Fat Mass and Subclinical

Atherosclerosis. *Arteriosclerosis, Thrombosis, and Vascular Biology* 2011; **31**(10)**:** 2322-2330.

35. Imhof BA, Aurrand-Lions M. Adhesion mechanisms regulating the migration of monocytes. *Nature Reviews Immunology* 2004; **4**(6)**:** 432-44.

36. Yowe D, Weich N, Prabhudas M *et al.* RGS18 is a myeloerythroid lineage-specific regulator of G-protein-signalling molecule highly expressed in megakaryocytes. *Biochemistry Journal* 2001; **359**(Pt 1)**:** 109-18.

37. Semplicini A, Lenzini L, Sartori M *et al.* Reduced expression of regulator of G-protein signaling 2 (RGS2) in hypertensive patients increases calcium mobilization and ERK1/2 phosphorylation induced by angiotensin II. *Journal of Hypertension* 2006; **24**(6)**:** 1115-24.

38. Pecht T, Haim Y, Bashan N *et al.* Circulating Blood Monocyte Subclasses and Lipid-Laden Adipose Tissue Macrophages in Human Obesity. *PLoS One* 2016; **11**(7)**:** e0159350.

39. Devevre EF, Renovato-Martins M, Clement K *et al*. Profiling of the three circulating monocyte subpopulations in human obesity. *Journal of Immunology* 2015; **194**(8)**:** 3917-23.

40. Ginhoux F, Jung S. Monocytes and macrophages: developmental pathways and tissue homeostasis. *Nature Reviews Immunology* 2014; **14**(6)**:** 392-404.

41. Swirski FK, Nahrendorf M, Etzrodt M *et al.* Identification of splenic reservoir monocytes and their deployment to inflammatory sites. *Science* 2009; **325**(5940)**:** 612-6.

42. Swirski FK, Nahrendorf M, Libby P. The ins and outs of inflammatory cells in atheromata. *Cell Metabolism* 2012; **15**(2)**:** 135-6.

43. Ortyn WE, Hall BE, George TC *et al.* Sensitivity measurement and compensation in spectral imaging. *Cytometry Part B: Clinical Cytometry* 2006; **69A**(8)**:** 852-862.

44. Wang L, Gaigalas AK, Marti G *et al*. Toward quantitative fluorescence measurements with multicolor flow cytometry. *Cytometry Part B: Clinical Cytometry* 2008; **73A**(4)**:** 279-288.

45. van der Meer AD, Vermeul K, Poot AA *et al*. Flow cytometric analysis of the uptake of low-density lipoprotein by endothelial cells in microfluidic channels. *Cytometry Part B: Clinical Cytometry* 2010; **77A**(10)**:** 971-975.

46. Jones NL, Reagan JW, Willingham MC. The pathogenesis of foam cell formation: modified LDL stimulates uptake of co-incubated LDL via macropinocytosis. *Arteriosclerosis, Thrombosis, and Vascular Biology* 2000; **20**(3)**:** 773-781.

Figure Legends

Figure 1

Cell surface expression of HLA-DR reveals heterogeneity of the intermediate monocyte subpopulations: Representative examples of 4 parameter (**A**) and 8 parameter (**B**) gating strategies used to identify three conventionally recognized monocyte subsets [classical (C), intermediate (Int) and non-classical (NC)] as well as two intermediate monocyte subpopulations (DR^{mid} (Mid) and DR^{hi} (Hi) intermediate) in freshly isolated PBMC from healthy adults. (**C**) Graphical representation of the results of monocyte sub-population analyses of PBMC from 8 healthy adults (5 female and 3 male) using 4 parameter and 8 parameter gating strategies. Monocyte sub-populations are expressed as proportions to the total monocyte population. Horizontal lines and error pars represent the mean ± SD while symbols represent values for the monocyte subpopulations from individual subjects.

Figure 2

Distinct surface phenotypes of monocyte subpopulations for chemokine receptors and adhesion proteins: Monocyte subpopulations were analyzed by the basic 4-parameter flow cytometry panel combined with antibodies against specific chemokine receptors **(A-E)** and adhesion molecule receptors **(F-L)**. Healthy adult PBMC samples were analyzed (CX3CR1 n=9, CCR2 n=12, CCR5 n=5, CCR6 n=5, CXCR4 n=4, CD11a n=5, CD11b n=5, CD11c n=9, CD49d n=5, CD62L n=5, PSGL-1 n=9, CD31 n=5). Horizontal lines and error pars represent the mean ± SD of the mean fluorescence intensity (MFI) while symbols represent MFI values for the monocyte sub-populations from individual subjects. Legend: C = Classical, M = DR^{mid} Intermediate, H = DR^{hi} Intermediate, NC = Non-Classical. *Statistical comparisons performed using ANOVA with Post Hoc Tukey's Test. ns = P > 0.05, * = P < 0.05; ** = P < 0.01; *** = P < 0.001. For "n = x", "x" is representative of replicate experiments.*

Figure 3

Chemokine-driven migration and endothelial adhesion and transmigration characteristics of monocyte subpopulations: **(A)** Representative dot plot demonstrating flow cytometric analysis of monocytes from the lower chamber of a transwell culture following migration toward medium alone (Resting) or medium containing CCL2 (Chemokine-induced). A greater number of events fall within the classical monocyte gate under chemokine-induced migration conditions. **(B)** Graphical representation of the index of migration of each of the four monocyte subpopulations in response to CCL2, CCL8 and CCL7 (data represented as mean ± SD for 8 replicate experiments, each performed with an individual PBMC sample from a healthy volunteer). **(C)** Graphical representation of the proportions of each of the four monocyte subpopulations within the floating (non-adherent), adherent and transmigrated fractions following addition of freshly-isolated PBMCs to transwells containing HAEC monolayers with (hatched columns) and without (solid columns) prior activation by TNFα (data represented as mean ± SD for 5 replicate experiments, each performed with an individual PBMC sample from a healthy volunteer). *Statistical comparisons performed using ANOVA with Post Hoc Tukey's Test. * P < 0.05; ** P < 0.01; *** P < 0.001. § P < 0.05 versus unstimulated, §§ P < 0.01 versus unstimulated. For "n = x", "x" is representative of replicate experiments.*

Figure 4

Comparison of intracellular calcium flux (Ca[i]) among monocyte sub-populations from healthy adults: **(A)** Representative examples of time-course of Ca[i] in classical (black) and DR^{mid} intermediate (red) monocytes in response to CCL2. **(B)** Representative examples of time-course of Ca[i] in DR^{hi} intermediate (blue) and non-Classical (green) monocytes. The dashed lines represent total monocyte Ca[i] in response to ionomycin (positive control). The arrow on the x-axis represents the time of CCL2 injection (30 seconds). **(C)** Indices of Ca[i] in monocyte sub-populations induced by ionomycin, carrier (0.1% BSA in Ca2+ free D-PBS) or CCL2. **(D)** Comparison of CCL2-induced indices of Ca[i] among the four monocytes sub-populations. Data for healthy adult PBMC samples. Data presented in C and D represent mean ± SD for 4 replicate experiments, each performed using PMBC from an individual healthy volunteer. *Statistical comparisons performed using two-sided*

paired t-test*. ns = P > 0.05, * = P < 0.05; ** = P < 0.01; *** = P < 0.001. For "n = x", "x" is representative of replicate experiments.*

Figure 5

Comparison of monocyte sub-population expression of regulator of G protein signaling (RGS) family members: Relative mRNA quantities in purified monocytes sub-populations from healthy adult PBMC samples for: **(A)** *RGS1*, **(B)** *RGS2*, **(C)** *RGS12*, **(D)** *RGS18*, **(E)** *FCG3RB* (CD16). *GAPDH* was used for normalization and classical monocytes as the reference sample. Legend: **C** = Classical, **M** = DR^{mid} intermediate , **H** = DR^{hi} intermediate, **NC** = Non-Classical monocytes. Horizontal lines and error pars represent the mean ± SD for each sub-populations while symbols represent values for individual subjects. A total of 7 replicate sorting experiments were performed using PBMC from individual healthy volunteers. Final qPCR results were obtained for 5-7 individual sorted samples for each target mRNA in each monocyte subpopulation. *Statistical comparisons performed using two-sided paired t*-test*. * = P < 0.05; ** = P < 0.01; *** = P < 0.001. For "n = x", "x" is representative of replicate experiments.*

Figure 6

DR^{mid} and DR^{hi} intermediate monocytes differ in their responses to modified lipoproteins: **(A)** Graphical representation of the surface expression levels of the scavenger receptors CD36 and SCAR-A, and the lipoprotein receptors LRP-1 and LDL-R on monocyte subpopulations of healthy adults as quantified by flow cytometric analysis. Results are presented as mean ± SD of the mean fluorescence intensity (MFI) for n=6 healthy volunteers. **(B)** Graphical representation of the uptake of unmodified LDL, oxidised LDL (oxLDL) and acetylated LDL (acLDL) by each monocyte subpopulation as quantified by flow cytometric analysis following incubation with Bodipy®-conjugated lipoprotein preparations. Results are presented as mean ± SD of the mean fluorescence intensity (MFI) for n=6 healthy adult samples. **(C)** Graphical representation of the migration of each

monocyte subpopulation across a 3 mM pore size membrane in response to oxLDL (25 μg/mL) and LDL (25 μg/mL) as quantified by 4-parameter flow cytometric analysis of migrated cells. The data shown represent the mean ± SD of the index of migration (experimental sample / control sample) results from 5 replicate experiments, each performed using PBMC from an individual healthy volunteer. Legend: C: Classical, M: DR^{mid} Intermediate, H: DR^{hi} Intermediate, NC: Non-Classical. *Statistical comparisons performed using ANOVA with Post Hoc Tukey's Test. * P < 0.05; ** P < 0.01; *** P < 0.001. § P < 0.05 versus unstimulated, §§ P < 0.01 versus unstimulated. For "n = x", "x" is representative of replicate experiments.*

Figure 7

DR^{mid} intermediate monocytes are selectively increased in number and proportion in adults with obesity compared to non-obese adults: **(A)** Graphical representation of total monocyte number per unit volume in healthy, non-obese (control) and obese adults as determined by the 4-parameter flow cytometry protocol. **(B)** Representative flow cytometry dot plots and graphical representation of 3-subset monocyte gating for PBMC samples of control and obese subjects (gated according to **Figure 1A**) which demonstrates differences in monocyte numbers and proportions for each of classical, intermediate and non-classical monocyte subpopulations. **(C)** Representative HLA-DR vs. CD16 dot plots and graphical representation of HLA-DR^{mid} and HLA-DR^{hi} expressing intermediate monocyte counts and proportions demonstrating selective increase in DR^{mid} intermediate monocytes in PBMCs of obese compared with control subjects (gated according to **Figure 1A**). All results are presented as mean ± SD for n=26 non-obese and n=18 obese. *Statistical comparisons performed using ANOVA with Post Hoc Tukey's Test. * P < 0.05; ** P < 0.01. For "n = x", "x" is representative of replicate experiments.*

Table 1: Clinical Characteristics and Demographic Details of Study Participants

	Control	OB	P value
Number	**33** (15 Female)	**42** (24 Female)	
Age (years)	**31** (22, 64)	**39.5** (21, 62)	**0.81**
Body Mass Index (kg/m^2)	**22.60** (18.0, 24.4)	**46.39** (30.34, 65.76)	**<0.0001**
Systolic Blood Pressure (mmHg)	**124.7** (122.5, 126.8)	**123.3** (122.5, 126.8)	**0.92**
Low Density Lipoprotein (mmol/L)	**2.18** (1.81, 2.54)	**3.01** (2.54, 3.47)	**0.04**
High Density Lipoprotein (mmol/L)	**2.12** (1.91, 2.34)	**1.24** (1.13, 1.36)	**0.01**
Triglycerides (mmol/L)	**0.74** (0.63, 0.85)	**1.60** (1.23, 1.99)	**0.008**
HbA1c (%)	**4.8** (4.6, 5.0)	**5.2** (5.1, 5.4)	**0.6**

Control: Healthy Individuals, BMI < $25kg/m^2$.

OB: Obese Individuals, BMI ≥ $30kg/m^2$ without type 2 diabetes.

Age & BMI expressed as Median with Range; All other data expressed as mean with 95% Confidence Intervals

Figure 1

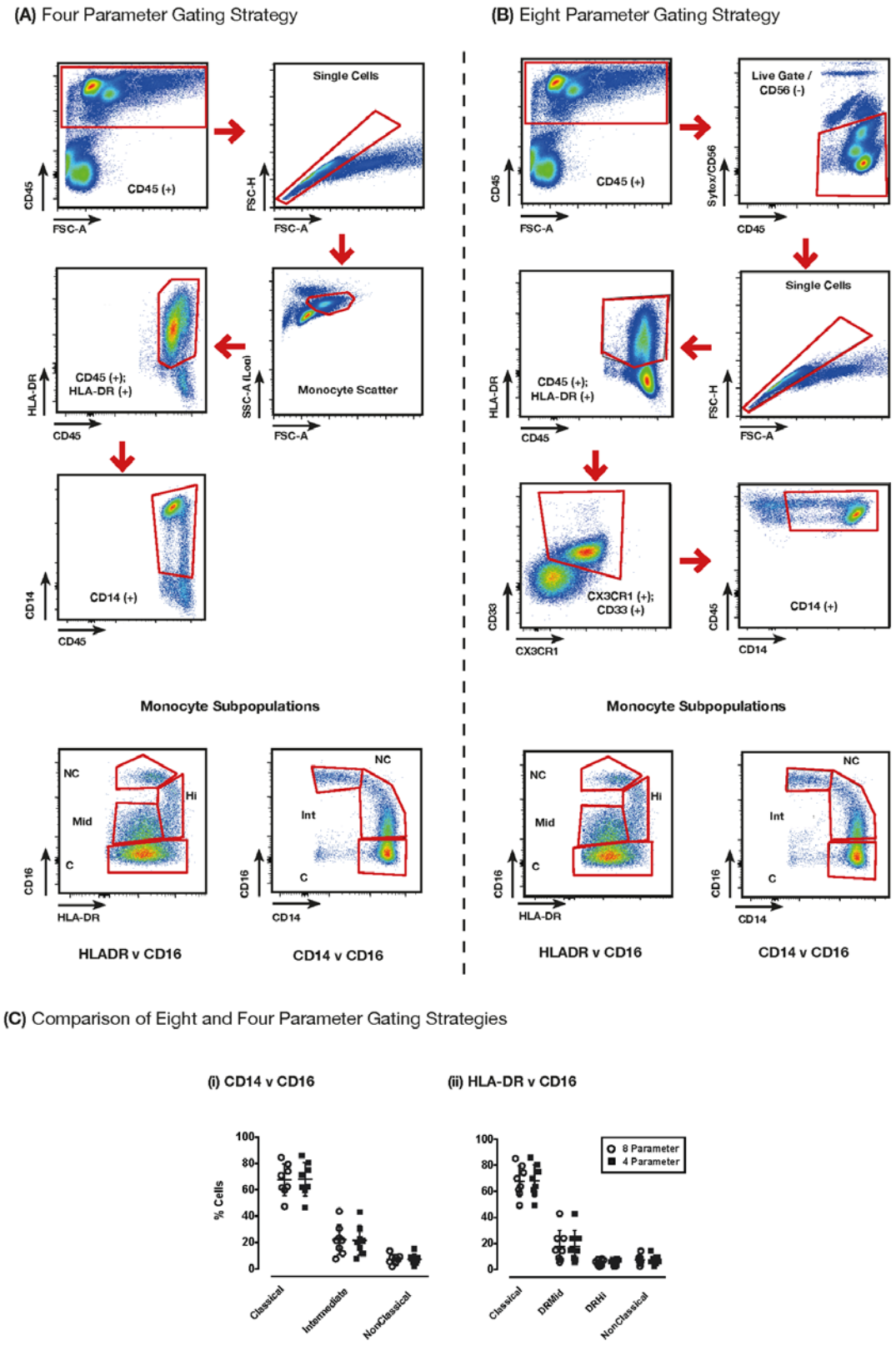
(A) Four Parameter Gating Strategy
(B) Eight Parameter Gating Strategy
CD45 (+)
Single Cells
Live Gate / CD56 (-)
CD45 (+); HLA-DR (+)
Monocyte Scatter
CD14 (+)
CX3CR1 (+); CD33 (+)
Monocyte Subpopulations
NC
Hi
Mid
Int
C
HLADR v CD16
CD14 v CD16

(C) Comparison of Eight and Four Parameter Gating Strategies
(i) CD14 v CD16
(ii) HLA-DR v CD16
% Cells
8 Parameter
4 Parameter
Classical
Intermediate
NonClassical
DRMid
DRNi

Figure 2

(i) Chemokine Receptors

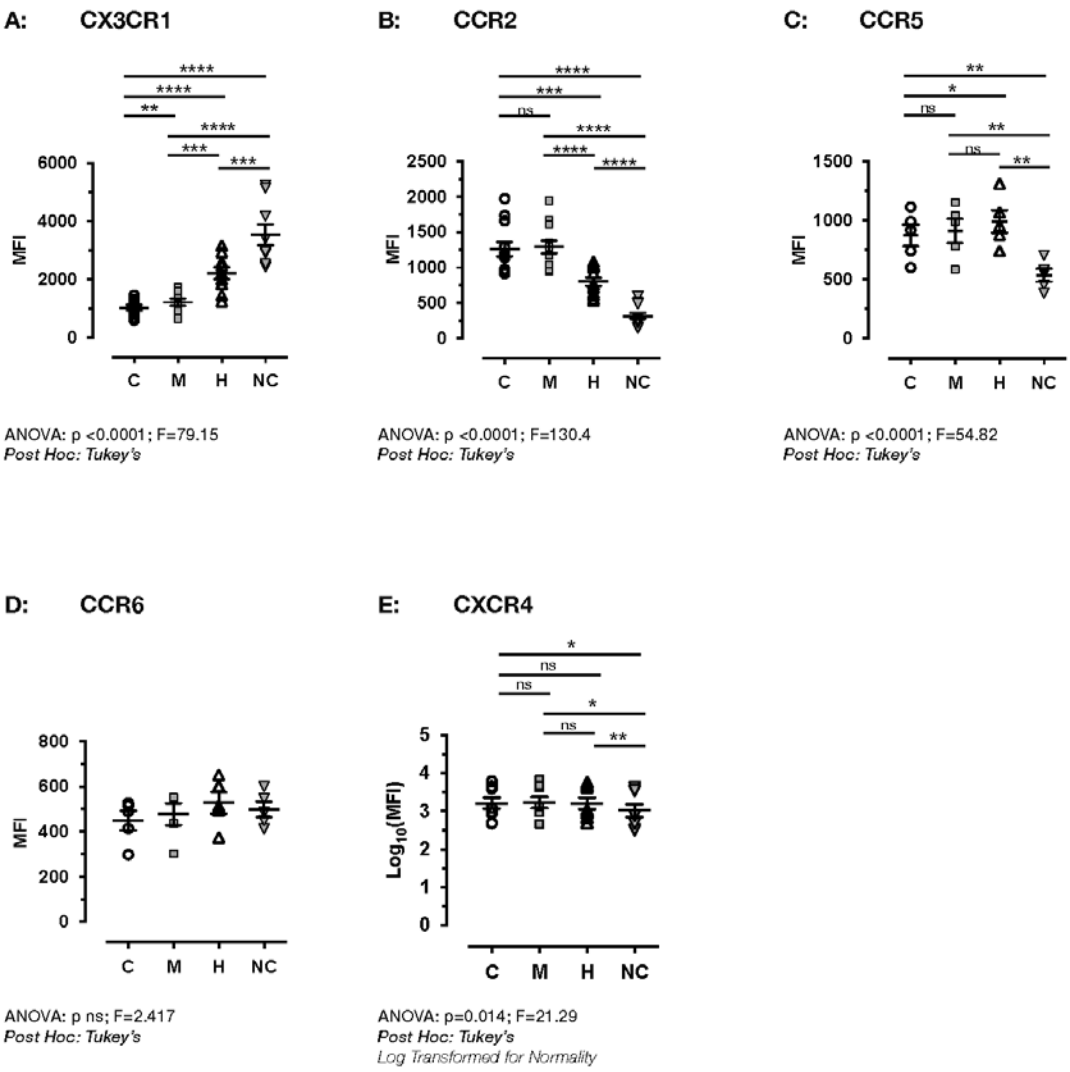

(ii) Adhesion Molecules

F: CD11a

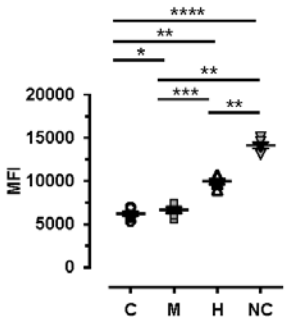

ANOVA: p <0.0001; F=260.0
Post Hoc: Tukey's

G: CD11b

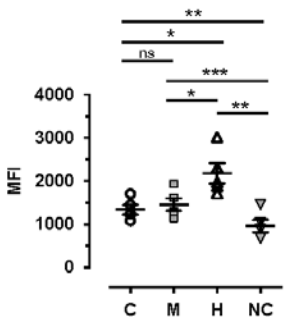

ANOVA: p=0.0004; F=61.98
Post Hoc: Tukey's

H: CD11c

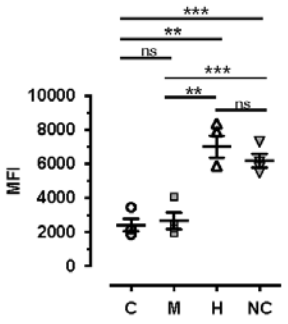

ANOVA: p=0.0004; F=122.0
Post Hoc: Tukey's

I: CD49d

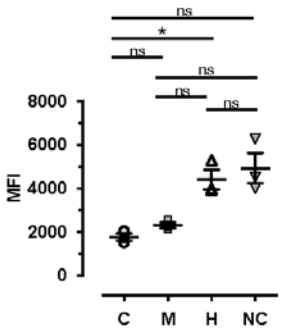

ANOVA: p=0.02; F=31.74
Post Hoc: Tukey's

J: CD62L

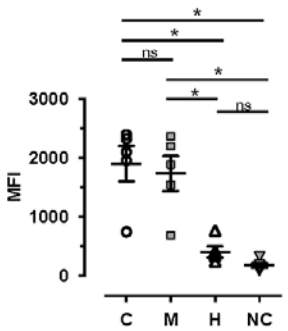

ANOVA: p=0.0033; F=30.68
Post Hoc: Tukey's

K: PSGL-1

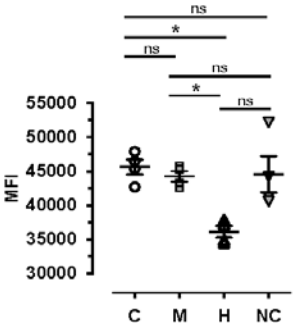

ANOVA: p=0.013; F=12.65
Post Hoc: Tukey's

L: CD31

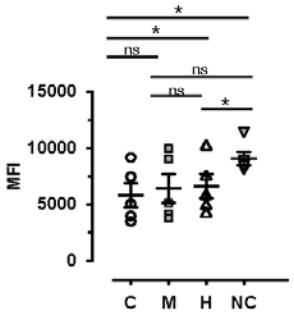

ANOVA: p=0.014; F=13.96
Post Hoc: Tukey's

Figure 3

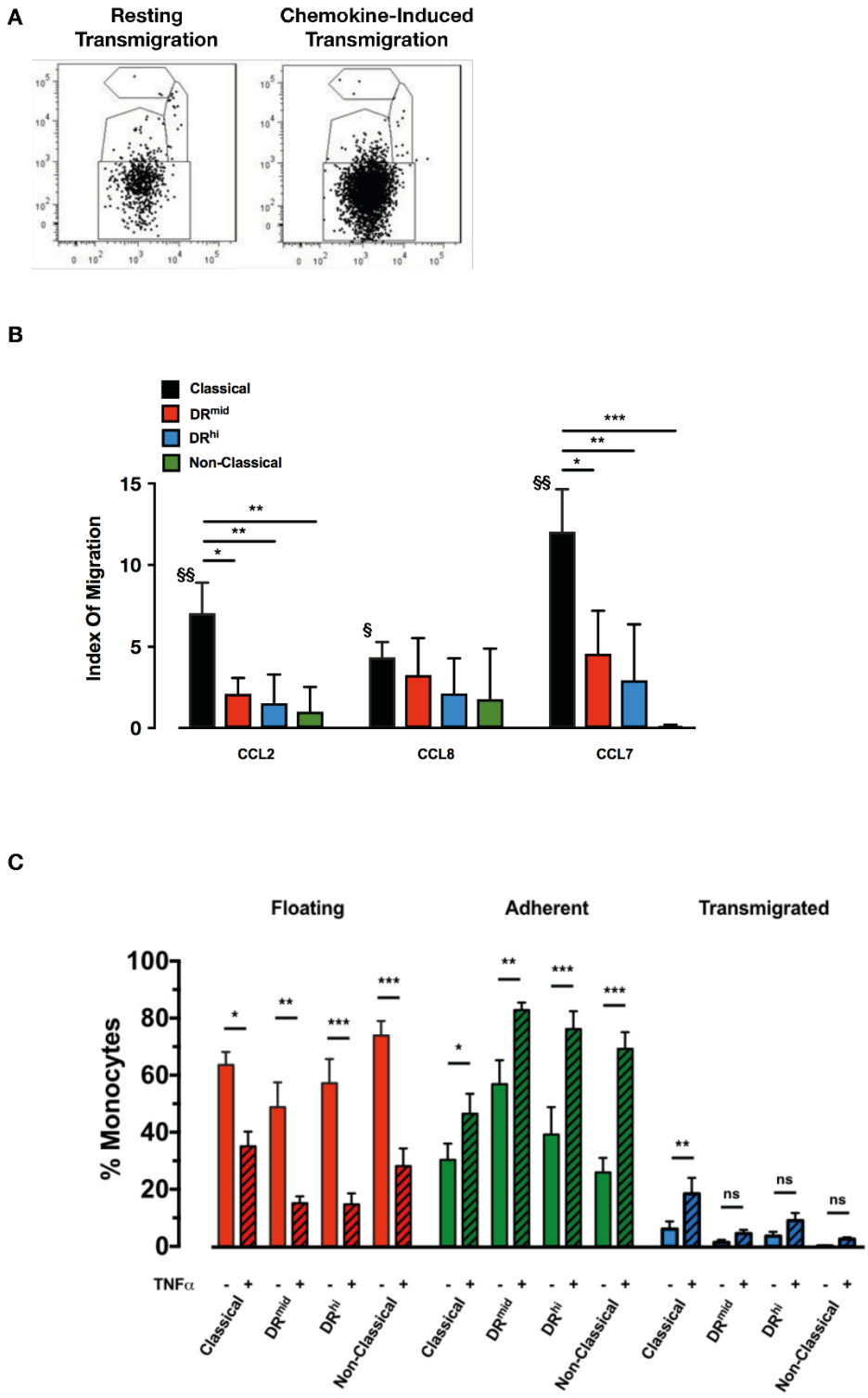
A
Resting Transmigration
Chemokine-Induced Transmigration
B
Classical
DRmid
DRhi
Non-Classical
Index Of Migration
CCL2
CCL8
CCL7
C
Floating
Adherent
Transmigrated
% Monocytes
TNFα
Classical
DRmid
DRhi
Non-Classical
ns

Figure 4

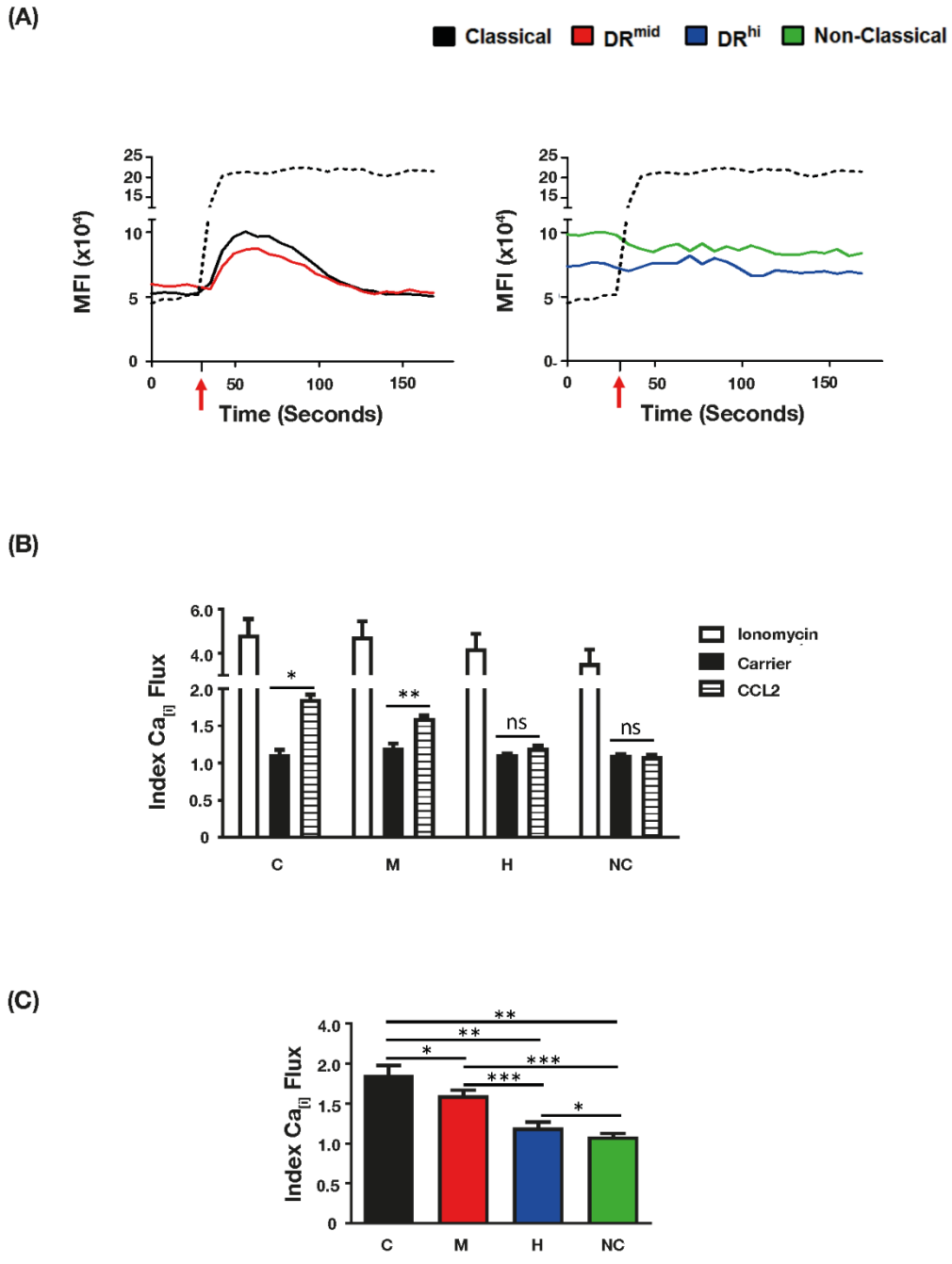
(A)
Classical
DR^mid
DR^hi
Non-Classical
MFI (x10^4)
Time (Seconds)
(B)
Index Ca[i] Flux
Ionomycin
Carrier
CCL2
C
M
H
NC
(C)
Index Ca[i] Flux
C
M
H
NC

Figure 5

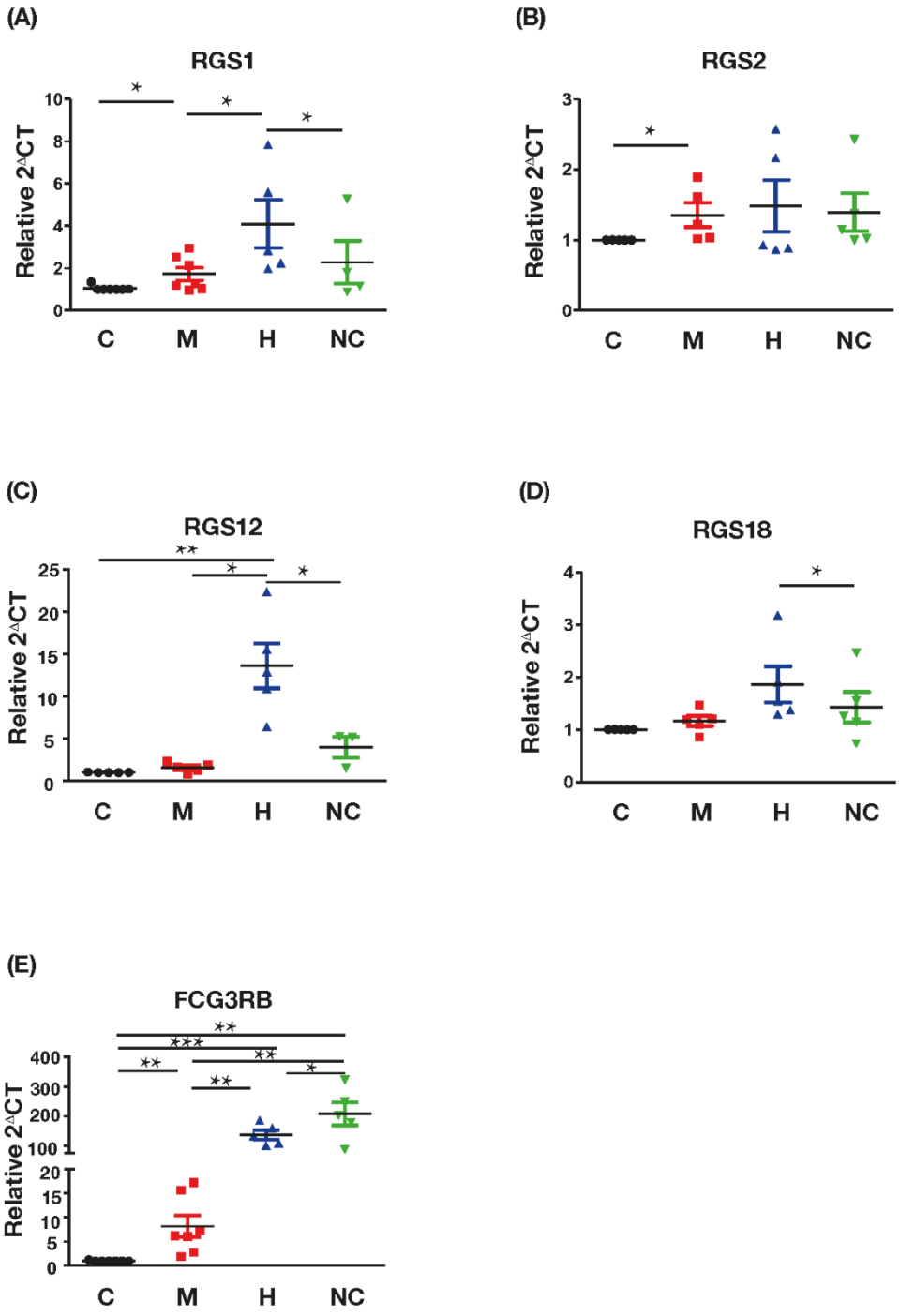
(A)
RGS1
Relative 2^ΔCT
C
M
H
NC
(B)
RGS2
Relative 2^ΔCT
C
M
H
NC
(C)
RGS12
Relative 2^ΔCT
C
M
H
NC
(D)
RGS18
Relative 2^ΔCT
C
M
H
NC
(E)
FCG3RB
Relative 2^ΔCT
C
M
H
NC

Figure 6

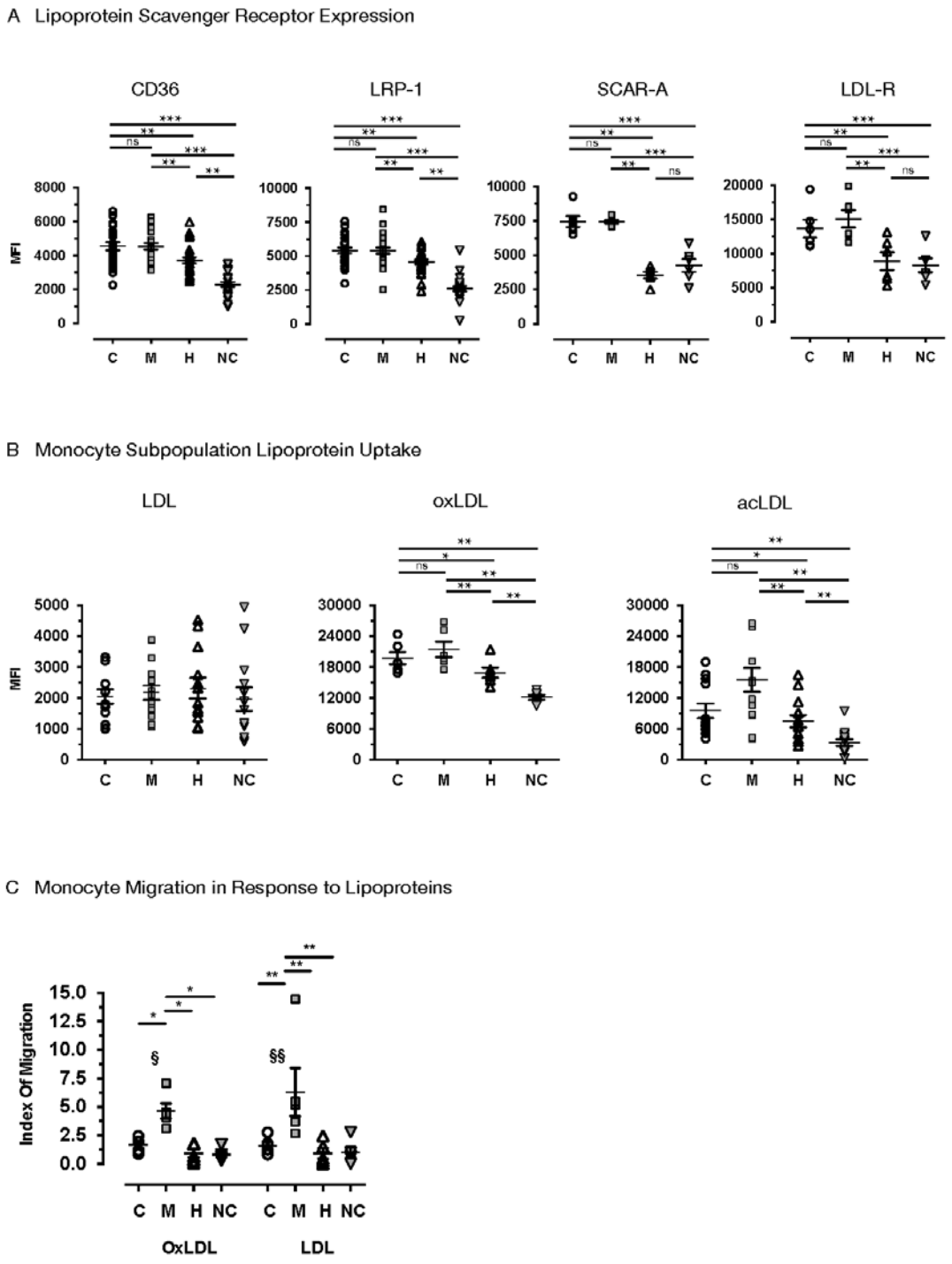
A Lipoprotein Scavenger Receptor Expression
CD36
LRP-1
SCAR-A
LDL-R
MFI
C M H NC
B Monocyte Subpopulation Lipoprotein Uptake
LDL
oxLDL
acLDL
C Monocyte Migration in Response to Lipoproteins
Index Of Migration
OxLDL
LDL

Figure 7

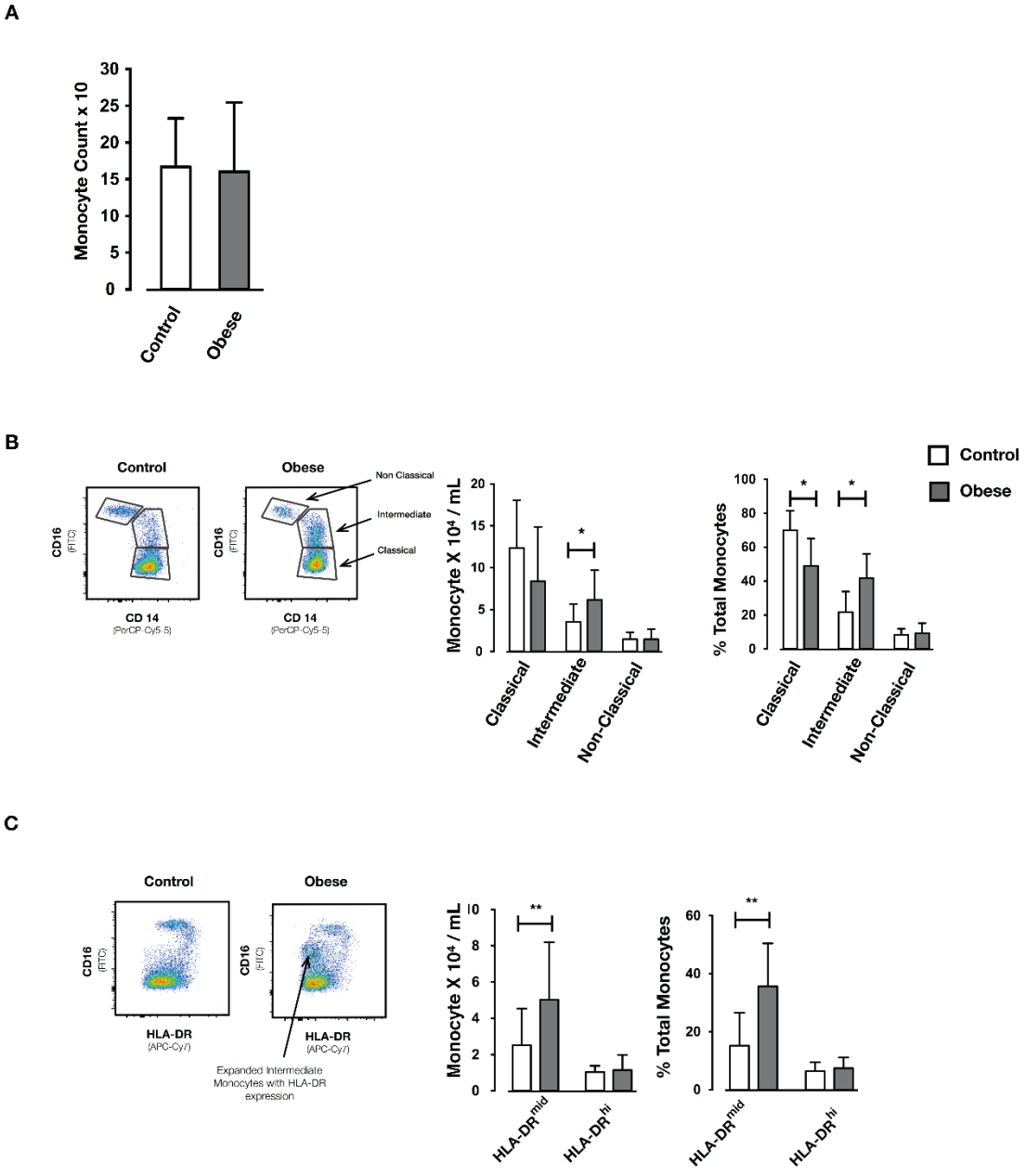
A
Monocyte Count x 10
30
25
20
15
10
5
0
Control
Obese
B
Control
Obese
Non Classical
Intermediate
Classical
CD16
(FITC)
CD 14
(PerCP-Cy5-5)
Monocyte X 10⁴ / mL
% Total Monocytes
Classical
Intermediate
Non-Classical
C
HLA-DR
(APC-Cy7)
Expanded Intermediate Monocytes with HLA-DR expression
HLA-DR^mid
HLA-DR^hi

Supplementary Figure 1: Cell surface expression of HLA-DR reveals heterogeneity of the intermediate monocyte subpopulations

A

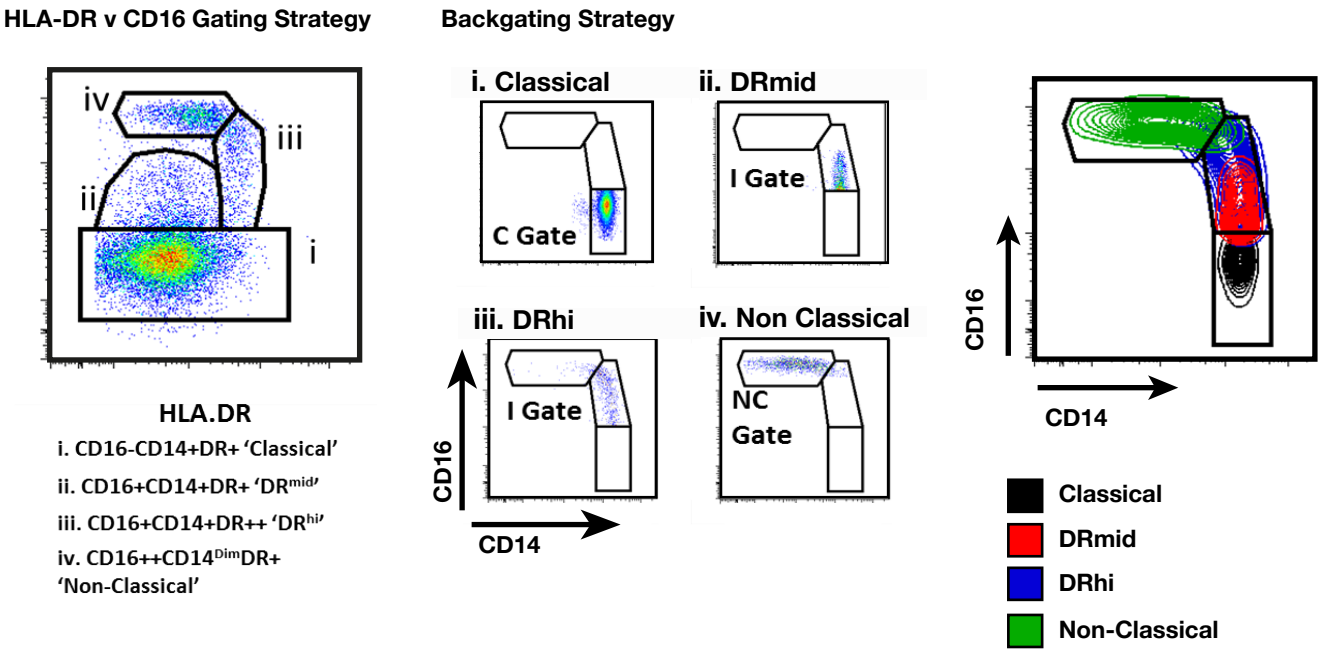

B

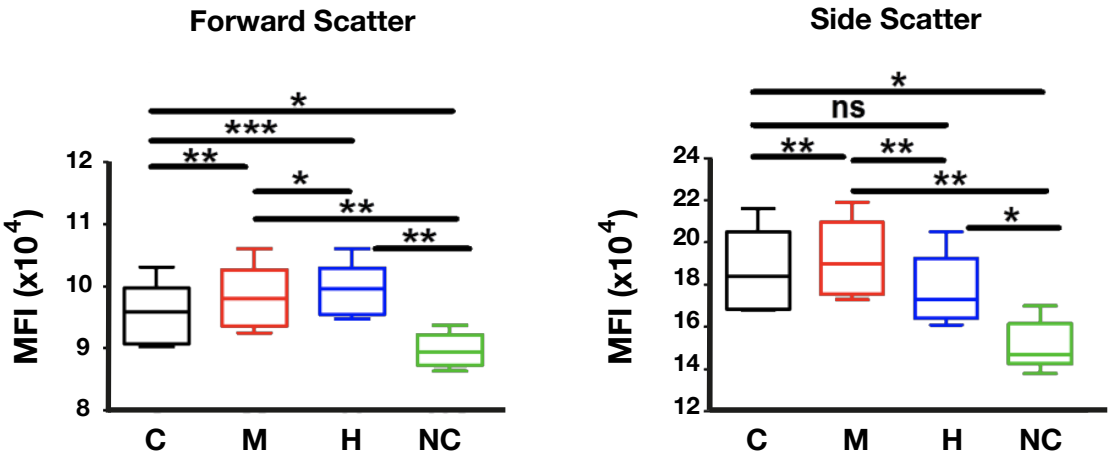

(A) Representative dot plots of the monocyte subpopulation gating used for the study. Using the 4 parameter gating strategy shown in Figure 1A, the final monocyte population is plotted using HLA-DR versus CD16, with separation of the intermediate monocytes according to their expression of HLA-DR into DRmid or DRhi subsets (left panel). Back-gating into CD14 versus CD16 dot plots demonstrates that both subsets fall within the intermediate monocyte population gate (mid and right panels). **(B)** Graphical representation of forward and side scatter measurements for each individual monocyte subpopulation including the DRmid and DRhi intermediate subsets based on 4-parameter analysis of PBMCs from healthy adult volunteers (n=8). Distinct scatter characteristics are demonstrated for each monocyte subpopulation (C:Classical; M: HLA-DRmid; H: HLA-DRhi; NC: Non-Classical) for both forward and side scatter. Statistical comparisons are made using the matched analysis of variance with Tukey's post hoc test. ns - non-significant; * $P < 0.05$; ** $P < 0.01$; *** $P < 0.001$.

Supplementary Figure 2: Human Aortic Endothelial Call Up-Regulation of Adhesion Molecules in response to TNFα

A

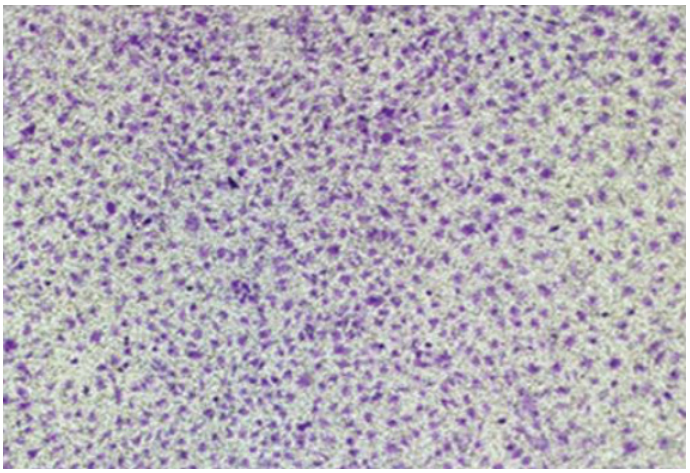

B

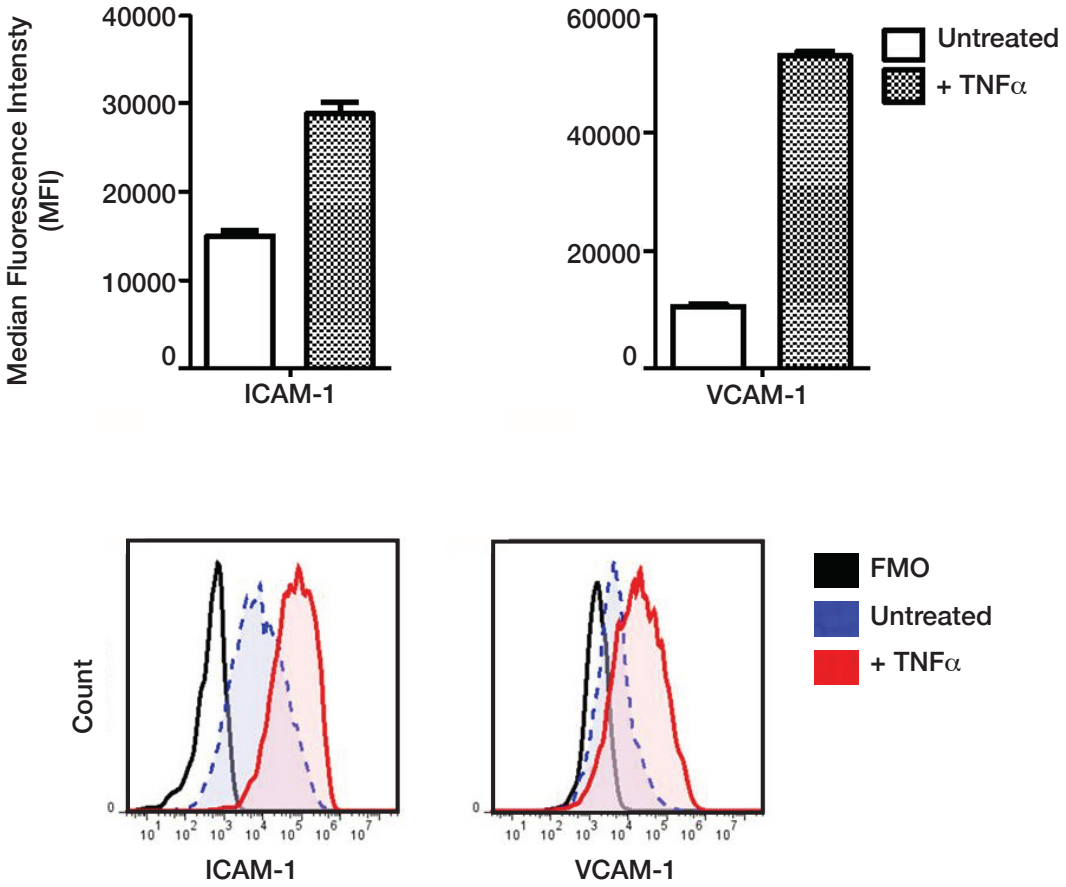

(A) Micrograph of a crystal violet stained confluent HAEC monolayer, seeded onto a fibronectin-coated Transwell® insert. **(B)** Surface expression of ICAM-1 and VCAM-1 in unstimulated and TNFα stimulated HAECs [analysed by flow cytometry (n=2)]. **(C)** Representative flow cytometry histograms of anti-ICAM-1 and anti-VCAM-1 stained HAECs under unstimulated versus TNFα-stimulated conditions. (FMO=Flow minus one control)

Supplementary Figure 3: Fluorescent Activated Cell Sorting of Human Monocyte Subpopulations.

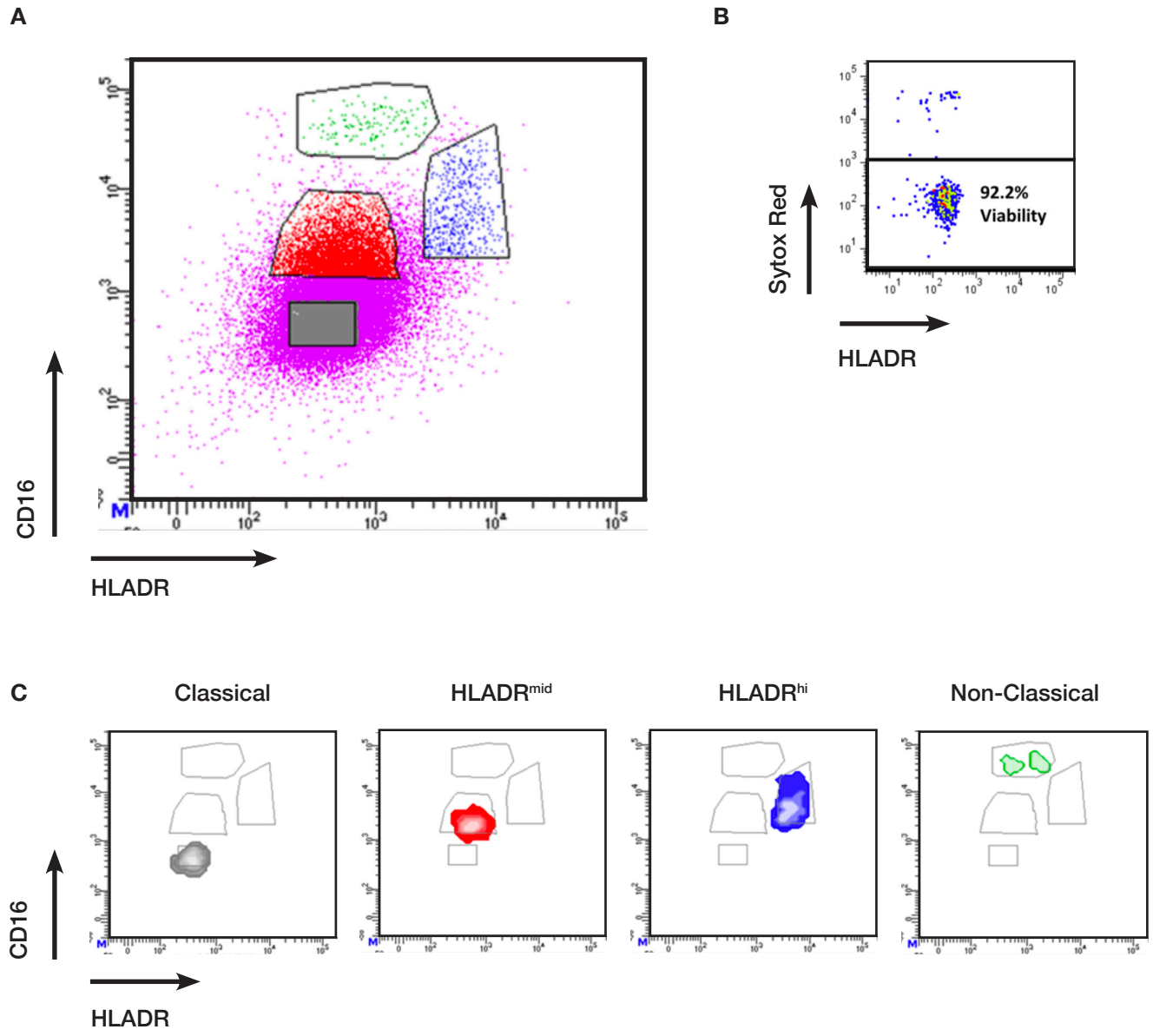

(A) Typical gate placement for FACS sorting of individual human monocyte subpopulations from PBMCs. **(B)** Representation of monocyte viability following sorting. **(C)** Represention of the purity of monocyte subsets following FACS sorting.

Supplementary Figure 4: Phenotype of individual monocyte subpopulations in obese and non-obese indivduals.

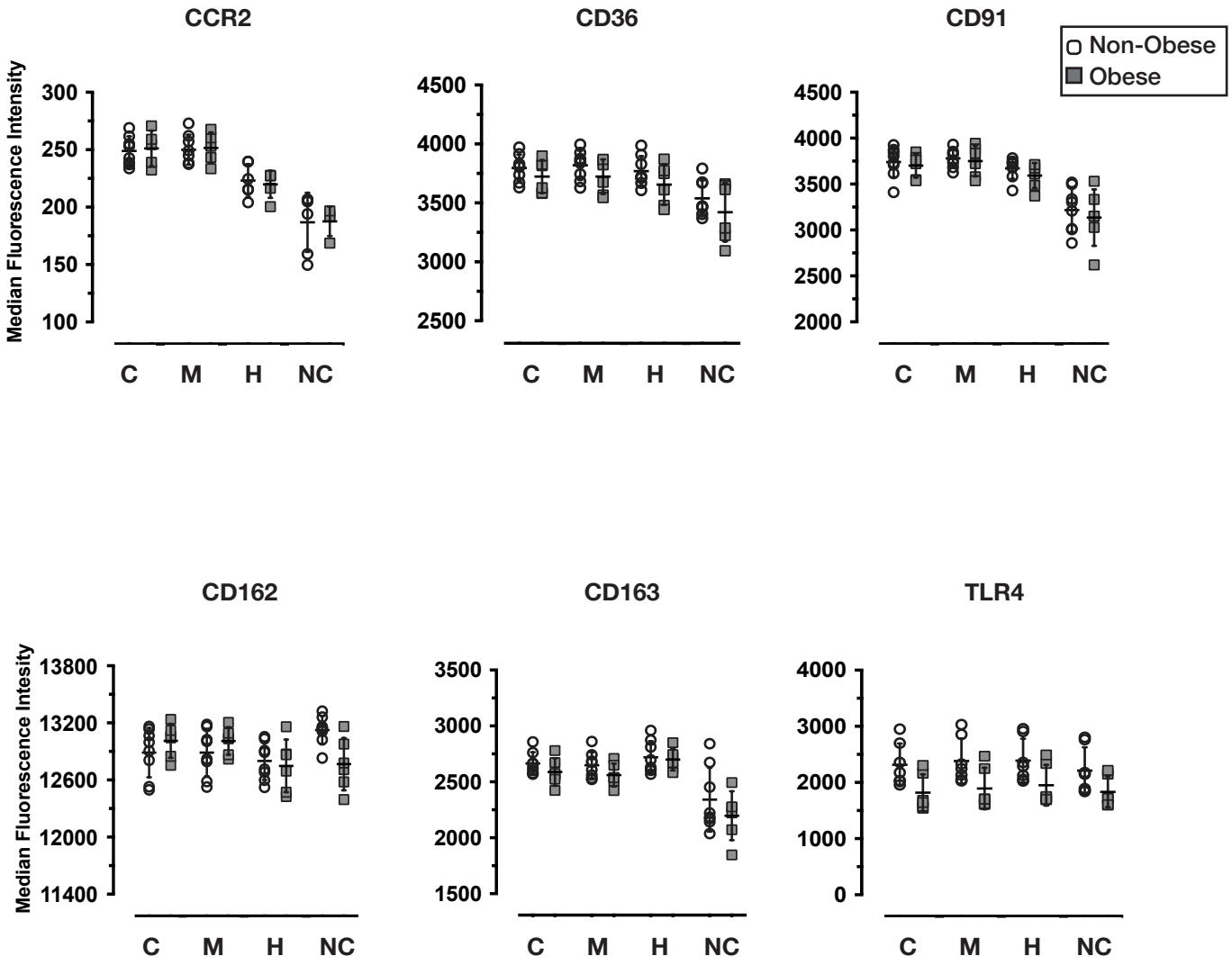

Cell surface phenotype measured by flow cytometry within individual human monocyte subpopulations did not differ for non-obese (open circle) and obese (grey boxes) individuals. There were no significant differences in the expression of the chemokine receptor CCR2, scavenger/lipoprotein receptors CD36, CD91 (LRP-1), CD162 (PSGL-1), CD163 or the inflammatory marker TLR4. (C: Classical; M: HLADR^{mid} Intermediate; H: HLADR^{hi} Intermediate; NC: Non-Classical).